Study of Sensing Issues in Dynamic Spectrum Access

Yuxian Ye

Thesis submitted to the Faculty of the
Virginia Polytechnic Institute and State University
in partial fulfillment of the requirements for the degree of

Master of Science
in
Computer Engineering

Yaling Yang, Chair
Y. Thomas Hou
A. Lynn Abbott

May 08, 2019
Blacksburg, Virginia

Keywords: Dynamic Spectrum Access, Spectrum monitoring, Energy harvesting, Energy management, Spectrum users' location privacy preserving

Study of Sensing Issues in Dynamic Spectrum Access

Yuxian Ye

(ABSTRACT)

Dynamic Spectrum Access (DSA) is now a commonly used spectrum sharing paradigm to mitigate the spectrum shortage problem. DSA technology allows unlicensed secondary users to access the unused frequency bands without interfering with the incumbent users. The key technical challenges in DSA systems lie in spectrum allocation problems and spectrum user's security issues. This thesis mainly focuses on spectrum monitoring technology in spectrum allocation and incumbent users' (IU) privacy issue.

Spectrum monitoring is a powerful tool in DSA to help commercial users to access the unused bands. We proposed a crowdsourcing-based unknown IU pattern monitoring scheme that leverages the power of masses of portable mobile devices to reduce the cost of the spectrum monitoring and demonstrate the ability of our system to capture not only the existing spectrum access patterns but also the unknown patterns where no historical spectrum information exist. Due to the energy limit of the battery-based system, we then leverage solar energy harvesting and develop an energy management scheme to support our spectrum monitoring system. We also provide best privacy-protection strategies for both static and mobile IUs in terms of hiding their true location under the detection of Environmental Sensing Capabilities system. In this thesis, the heuristic approach for our mathematical formulations and simulation results are described in detail. The simulation results show our spectrum monitoring system can obtain a high spectrum monitoring coverage and low energy consumption. Our IU privacy scheme provides great protection for IU's location privacy.

Study of Sensing Issues in Dynamic Spectrum Access

Yuxian Ye

(GENERAL AUDIENCE ABSTRACT)

Spectrum relates to the radio frequencies allocated to the federal users and commercial users for communication over the airwaves. It is a sovereign asset that is overseen by the government in each country to manage the radio spectrum and issue spectrum licenses. In addition, spectrum bands are utilized for various purposes because different bands have different characteristics. However, the overly crowded US frequency allocation chart shows the scarcity of usable radio frequencies. The actual spectrum usage measurements reflect that multiple prized spectrum bands lay idle at most time and location, which indicates that the spectrum shortage is caused by the spectrum management policies rather than the physical scarcity of available frequencies.

Dynamic spectrum access (DSA) was proposed as a new paradigm of spectrum sharing that allows commercial users to access the abundant white spaces in the licensed spectrum bands to mitigate the spectrum shortage problem and increase spectrum utilization. In DSA, two of the key technical challenges lie in how to dynamically allocate the spectrum and how to protect spectrum users' security. This thesis focuses on the development of two types of mechanisms for addressing the above two challenges: (1) developing efficient spectrum monitoring schemes to help secondary users (SU) to accurately and dynamically access the white space in spectrum allocation and (2) developing privacy preservation schemes for incumbent users (IU) to protect their location privacy. Specifically, we proposed an unknown IU pattern monitoring scheme that leverages the power of masses of portable mobile devices to reduce the cost of common spectrum monitoring systems. We demonstrate that our system can track not only the existing IU spectrum access patterns but also the unknown patterns where no historical spectrum information exists. We then leverage the solar energy harvesting and design energy management scheme to support our spectrum monitoring system. Finally, we provide a strategy for both static and mobile IUs to hide their true location under the monitoring of Environmental Sensing Capabilities systems.

Dedication

I dedicate this thesis to my parents and grandparents who I love the most.

Acknowledgments

First of all, I would like to sincerely give thanks to my advisor Dr. Yaling Yang for giving me tremendous support and guidance on research. I started from scratch in the field of networking when I joined our Lab. She has put forward novel ideas, listened carefully to my thoughts, and given good advice. It was her patient guidance that helped me through the hard times. This thesis would have not even been completed without her. I would once again greatly appreciate her encouragement during the past two years. She is not only an incredible research advisor but also an amazing mentor during my life.

Secondly, I would also like to thank Dr. Hou, Y. Thomas and Dr. A. Lynn Abbott for being my committee and taking their time to attend my thesis defense.

Thirdly, I would like to thank Yousi Lin, the Ph.D. student in our lab, who has helped me a lot on research. Thanks for her patience in giving me suggestions on solving mathematical and experimental problems.

Lastly, I am very grateful to Virginia Tech and Shandong University for giving me a good education, which will have a positive impact on me in the future.

Contents

List of Figures

List of Tables

Chapter 1

Introduction

1.1 Dynamic Spectrum Access

In the past few decades, it has been widely believed that our available radio frequencies are running out. The overcrowded radio frequency allocation chart in the US (Figure 1.1) also strongly proves it. However, the Federal Communications Commission (FCC) Spectrum Policy Task Force [3] gives an actual spectrum usage observation: Some spectrum frequency bands (e.g., television broadcasting) have continuous occupation, while a great deal of the precious spectrum is idle at any given time and location. This paradox indicates that spectrum shortage is caused by spectrum management policies rather than the physical scarcity of available frequencies [4]. Traditionally, unshared fixed access of fixed bands are given to the licensed users which has resulted in little spectrum available for allocation to emerging communication technologies and requirements. On the other hand, many licensed bands are not fully utilized in both time and frequency domains, which are called spectrum holes or white spaces [5]. These unshared bands provide a good opportunity for wireless communication. Therefore, the underutilization of spectrum has stimulated people to actively seek

better spectrum management methods and policies, among which Dynamic Spectrum Access (DSA) is a commonly used spectrum sharing paradigm to mitigate this problem. In DSA, the secondary users (SUs) dynamically search for idle spectrum bands and are allowed to opportunistically access the white spaces in the licensed spectrum bands for wireless communications [5]. In order to avoid triggering any harmful interference to the incumbent users' communications, SUs need to continuously monitor the spectrum while yielding to incumbent users. In this way, DSA can moderate spectrum scarcity and utilize a large quantity of underutilized spectrum [6].

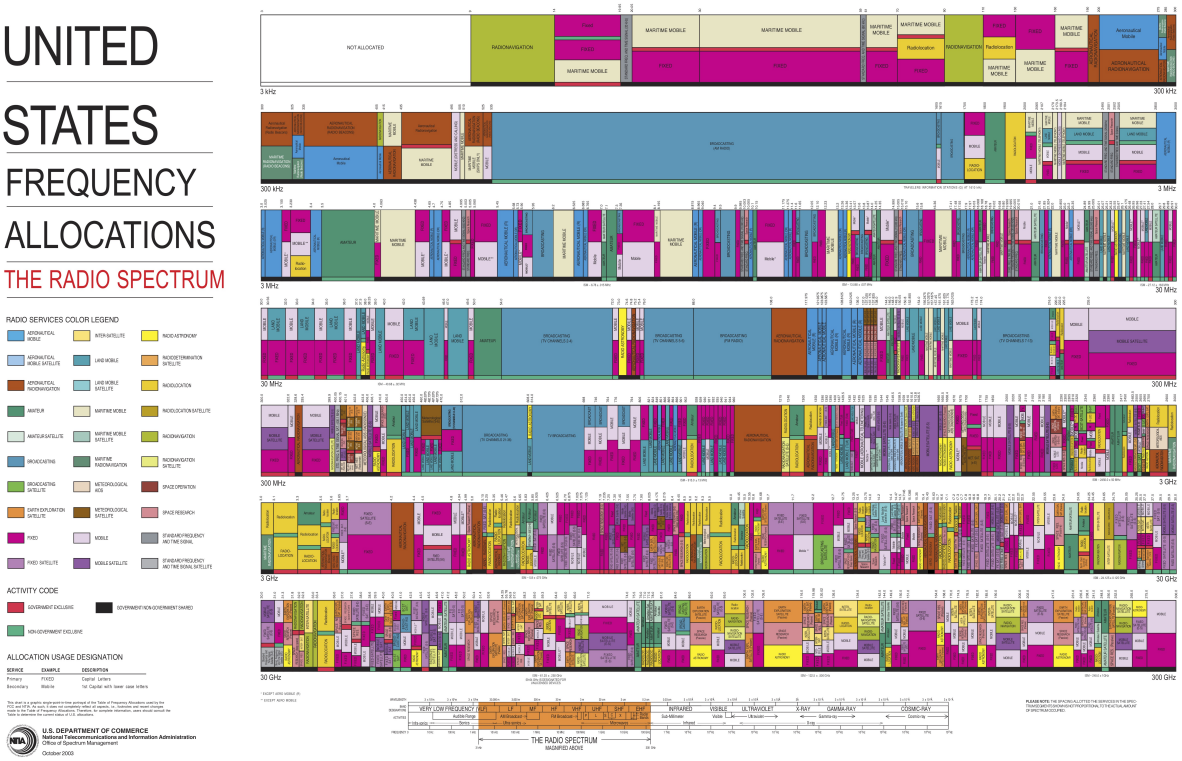

Figure 1.1: US frequency Allocation Chart[1]

1.2 Sensing Issues in DSA

Dynamic Spectrum Access technology has aroused widespread attention because it has become a crucial solution to spectrum shortage problems [5]. The main structure of current Dynamic Spectrum Access system is shown in Figure 1.2. In DSA, the SUs can opportunistically access the spectrum white spaces as long as they do not trigger any harmful interference to the IUs' communication. The Environmental Sensing Capability (ESC) system is usually utilized in spectrum sharing in the 3.5 GHz band to detect the presence of incumbent shipborne radar systems and trigger protection [7]. It can detect the incumbent users' (IU) activities for protecting them from SUs' interference as well as maximizing secondary spectrum usage. Spectrum Access System (SAS) Server (shown in Figure 1.2 part B) is a cloud-based spectrum management infrastructure which is set up for allocating spectrum resources according to interference management method and protecting the operation of incumbent and secondary users [8]. After detecting the presence of incumbent federal systems in particular bands, the ESC communicates the presence of IU signal to one or more SAS-Server while triggering protective measures. The SAS-Server then is able to appropriately allocate SUs to utilize the white spaces.

Two of the key technical challenges of sensing issues that are being explored in current dynamic spectrum systems lie in spectrum allocation problems and spectrum users' security issues [9, 10]. In the following parts, I will introduce the critical technologies and the sensing issues that this thesis focuses on.

As discussed in section 1.1, current wireless network is characterized by the government's static spectrum allocation strategy. During allocation process, spectrum monitoring is the key role to monitor real-time spectrum utilization. Thus, spectrum monitoring is a powerful tool in Dynamic Spectrum Access to help SUs timely and accurately access the unused

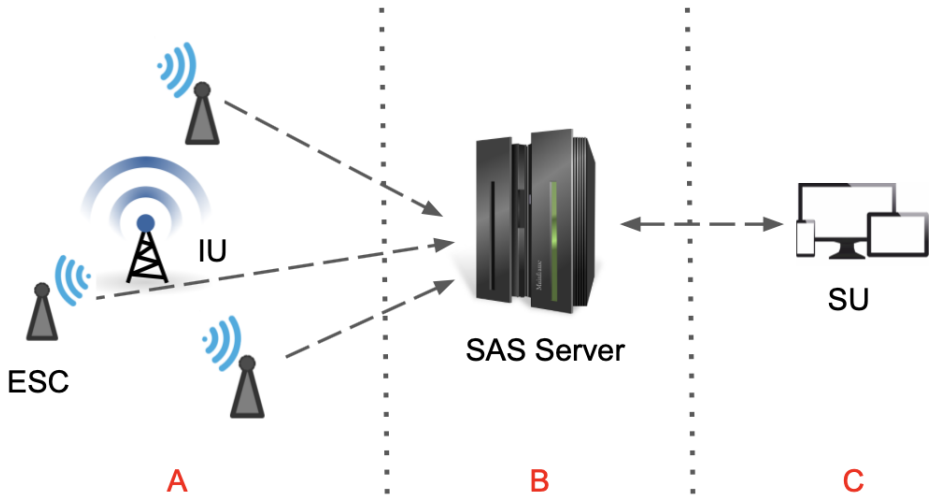

Figure 1.2: Overview of dynamic spectrum access system. This thesis focus on leveraging the SUs in part "C" to monitor spectrum in part "A", and IU Location privacy preserving scheme against Environmental Sensing Capabilities in part "A".

spectrum white spaces. It is also one of the two technologies that this thesis examines. As shown in Figure 1.2 part A, in order to monitor the spectrum of IU, a traditional spectrum monitoring system leverages some dedicated spectrum observatories and stations to keep scanning the spectrum and extract useful information, which will be finally stored in various spectrum databases, to obtain detailed spectrum occupancy information. Since today's spectrum facilities cost too much to build and have low geographic coverage, we consider to leverage the power of masses of portable mobile users (see Figure 1.2 part C) to address the current limitations and design a crowdsourcing-based spectrum monitoring system. In chapter 2 of this thesis, we demonstrate the ability of our system to capture not only the existing spectrum access patterns but also the unknown patterns where no historical spectrum information exists.

Since our system needs to frequently scan the spectrum, the system can burden battery energy conservation[11]. A system composed of a large number of spectrum sensors may run out of their energy at the end of the day. Because of that, in chapter 3 of this thesis, we

investigate solar energy harvesting to mitigate the energy scarcity problem.

From the perspective of security, most of the existing research on DSA systems assumes that the participants involved are honest, while recent research shows that DSA systems still have major security challenges (e.g., DoS attacks, spoofing, data modification, etc.) [9]. Among them, a critical issue is IUs' location privacy in 3.5 GHz. Most of the existing IU location privacy protection related works either add noise or distortion on IU location data, or encrypt the location data by homomorphic cryptosystem before transmit data to SAS system[12–15] which is used to grant spectrum access permissions to SUs based on the location and communication activities of IUs (see Figure 1.2 part B). However, these designs are not applicable in 3.5 GHz DSA system because IU location data is not sent to SAS in 3.5 GHz.

On the one hand, SAS system must leverage the exact location and transmission activity information of IUs to accurately grant SUs spectrum access permissions. On the other hand, the 3.5 GHz band is mostly reserved for military systems, like U.S. naval radars. Due to the sensitivity of the IUs' location, directly revealing IUs' location information to the SAS will compromise incumbents operational security (OPSEC). These conflicting requirements pose a huge challenge for designing Citizens Broadband Radio Service (CBRS) which is promulgated by FCC for spectrum sharing between government incumbents and commercial wireless broadband users in the 3500-3700 MHz (referred to as 3.5 GHz band) [16, 17]. In this way, Wireless Innovation Forum (WINNF) has been developing requirements to preserve OPSEC as required by FCC for operation in the 3.5GHz band [18] from 2015. It is currently proposed to use Environmental Sensing Capability (ESC) systems to mitigate the challenge of OPSEC by measuring the received signal strength (RSS) of IU signal and provide such information to SAS. However, it is not security enough since ESC still sends IU sensing results (RSS) to SAS, which gives the potential adversary reliable information. Since whether federal

privacy issues can be solved affects the benefits of spectrum sharing between government IUs and commercial SUs, we seek to find an effective way to protect IU's location privacy under these circumstances.

1.3 General Motivation and Contribution

Based on the sensing issues in DSA, the motivation of our research works are try to overcome some of the challenges on both spectrum allocation problems and security issues. Including improving existing spectrum monitoring schemes based on mobile devises and adjusting the energy supplement scheme to solar energy harvesting in order to prolong system's life. We also present a theoretical analysis on the feasibility of preserving both static and moving IU's location information and how it is affected by adjusting IU's radiation pattern and transmit power.

The contribution of this thesis are as follows:

- We designed a crowdsourcing-based spectrum monitoring system which can intelligently schedule the monitoring tasks for masses of portable mobile devices by leveraging the IU occupancy patterns. Based on previous existing IU pattern monitoring algorithms that done by the Ph.D. student in our group, in this thesis, I proposed an unknown IU pattern monitoring scheme which is able to discover new IU transmission activities that are not included in recorded database. The unknown pattern monitoring algorithm ensures our system can start to function even when no historical data is provided.

- As time proceeds, the battery-based spectrum monitoring system will be exhausted and the sensor will shut down. To alleviate such problems and prolong system life, I

proposed a solar energy prediction Long short-term memory recurrent neural network to accurately predict future incoming solar power and design a heuristic algorithm based on solar energy harvesting which can intelligently schedule the monitoring tasks by leveraging the spectrum occupancy patterns. The new power management scheme guarantees our system's functionality no matter whether there is any harvestable solar power or not.

- In this thesis, we show the heuristic algorithm and simulation results for our protection scheme. To hide the IUs' location information under the detection of ESCs, our group presented a theoretical analysis on the feasibility of preserving both static and moving IUs' location information and how it is affected by adjusting IU's radiation pattern and transmit power. In this cooperation work, the Ph.D. student in our group formulated the problem for both static IUs and moving IUs. One of the contribution of my work in this thesis is the heuristic approach based on sampling to solve our intractable mathematical formulations. Another contribution is the simulation for both static IU and moving IU. The simulation results show that our approach provides great protection for IU's location privacy.

Chapter 2

Crowdsourcing-based Unknown IU Pattern Monitoring

2.1 Introduction

2.1.1 Spectrum Monitoring

A commonly used method to dynamically obtain spectrum availability information for the SUs is spectrum monitoring. Spectrum monitoring is a reliable tool for planning and using frequencies, avoiding incompatible usage, and identifying sources of harmful interference. The technologies of spectrum monitoring include automatic signal detection and analysis, in-band interference detection and signal characterization, etc. There are some special spectrum monitoring observatories and stations, such as Microsoft spectrum observatory, showing detailed spectrum occupancy information temporally and spatially. Such systems extract useful information by keep scanning the spectrum and finally store them in several kinds of spectrum databases. The type of useful information that we extracted is commonly referred

to the spectrum occupancy pattern. Each pattern represents a spectrum utilization block in both time and frequency domain to represent the behavior of the corresponding incumbent user.

Nevertheless, existing systems and monitoring approaches have conclusive drawbacks. Firstly, spectrum observatories are not widely deployed and are mostly installed by the government or well-funded enterprises. The reason is that the hardware is too costly and cumbersome to operate and maintain. Secondly, most existing methods are inefficient and naive because they only scan the spectrum in sequence. Thirdly, some other systems focus on the intelligent task scheduling of a single spectrum monitoring sensor [19]. There are still others have proposed multi-sensor coordination for spectrum monitoring to reduce costs [20]. These traditional methods require plenty of time to build infrastructure and manpower to manipulate. Moreover, there is no cheap, stable and effective detection system was proposed.

2.1.2 Crowdsourcing

There is a tantalizing question: What if the solutions of the greatest problem weren't waiting to be conceived, but already existed somewhere in the world? This is why the concept of Crowdsourcing is elicited [21]. Crowdsourcing refers to a task performed by a designated agent and is outsourced by publicly calling an undefined but large group of people. It allows the power of the crowd to complete tasks that were once only belonged to the minority. In other words, crowdsourcing takes the principles that apply to open source software projects and applies them to a wide range of areas. In software engineering, crowdsourcing also has been widely used. For example, Amazon Mechanical Turk [22] leverages one kind of the crowdsourcing called micro-tasking. Whether it is software development, software testing, or simply sharing knowledge, crowdsourcing can make good use of the power and wisdom of the crowd to complete.

In our scheme, we propose to leverage the power of crowdsourcing to address current limitations. Especially, the mobile SUs in our research is utilized as not only users of available spectrum white space but also moving spectrum monitoring devices. In this way, we could achieve low-cost spectrum monitoring at a large geographical scale with a central controller which coordinates a great number of secondary mobile devices. There are two principal challenges in the design of the crowdsourcing-based spectrum monitoring system: limited energy and dynamics in crowd distribution. In our system, it is obvious that mobile users, such as cell phones, have their own daily application routines. When we use these mobile users for spectrum monitoring, we must first ensure that the monitor process should not disturb their normal manipulation. Therefore, the remaining energy available for spectrum monitoring is also limited. In addition, an important feature of mobile users is mobility. The number of devices in a particular area that can be used to monitor the spectrum varies at different times and may result in a temporary shortage of the number of local devices. Therefore, the difficulty lies in how to use the limited energy and the ever-changing number of mobile users to achieve the highest spectrum monitoring coverage.

In order to overcome these difficulties, our strategy is to leverage the IU occupancy pattern. We used the IU pattern record in the Cityscape Spectrum Observatory [2] database as experimental data. As shown in Figure 2.1, the actual spectrum access behavior can show a clear pattern. The light parts refer to the representation of IU activities in spectrum. The dark parts represent the unused spectrum. Thus, the recorded past spectrum dataset can be used not only to extract past spectrum access patterns but also to imply future dynamics in spectrum access. Our spectrum monitoring system is designed with intelligent scheduling algorithms to discover dynamic patterns of past spectrum activity to improve monitoring efficiency and reduce energy consumption within the system.

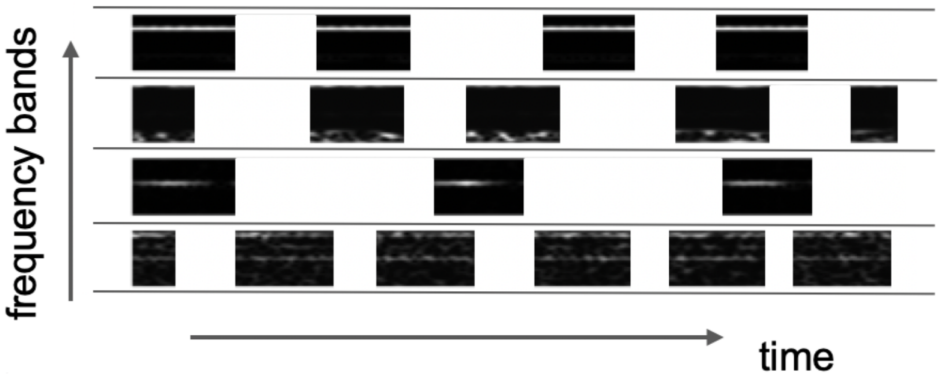

Figure 2.1: Four examples of past IU patterns (frequency bands) used in our experiment from Cityscape Spectrum Observatory [2]. X axis refers to time variation.

2.1.3 Motivation

Our previous works have already mandated SUs to monitor the IU patterns that have occurred in the past. Nonetheless, the historical information will grow inaccurate as time goes by due to IUs' spectrum access behavior change and mobility, which will finally degrade the performance of our proposed system. To keep our system updated with the dynamic spectrum, we also need to discover new IU patterns.

2.1.4 Contribution

In previous research on dynamic spectrum monitoring, the common approach is costly and naive because their approach is to build infrastructures (e.g., spectrum observatories) and merely scan the spectrum sequentially. To aid in this, we proposed a crowdsourcing based spectrum monitoring system at a large geographical area that leverages the power of masses of portable mobile device to monitor the existing IU patterns.

In this work, the focus lies on how we discover new patterns and model the distribution of

new occurrence intervals. We design a scheme to discover IU transmission activities that are not included in existing recorded database. our system includes an intelligent algorithm that observes and learns new patterns not found in history. Our experiment results reflect that our system achieves a high spectrum monitoring coverage and does not require any additional infrastructure which is more efficient than traditional monitoring system. With the unknown IU pattern monitoring scheme, our system gain the ability of scheduling from scratch, which means it ensures that our system can start to function even when no historical data is provided. It gradually create the pattern dataset and improve its monitoring intelligence based on the historical data. This ability makes our system more effective and more adaptive to different geographical areas compared with other spectrum monitoring systems.

2.2 Background

2.2.1 Related Works

The existing crowdsourcing spectrum monitoring research works can be categorized into two parts. One part of existing research works focus on the hardware implementation. For example, [20] performed detailed hardware platform using smart phones and RIL dongles. [23] leverage crowdsourced mobile hardware to collect spectrum measurements in a large scale and [24] designed sensors upon a low-cost commercial off-the-shelf (COTS) platform. These studies leverage commodity mobile devices to build hardware platforms for distributed spectrum monitoring systems. However, they do not address the approaches to manage their systems for optimal monitoring performance.

The other part of existing spectrum monitoring works assume spectrum sensors are dedicated and fixed devices. For instance, the sensor cooperation scheme of CityScape [2] and an end-

to-end system Spectrum Observatory [25] are simply let each sensor scan the spectrum in sequentially. SpecInsight [19], a real-time system acquiring view of 4 GHz of spectrum, is an expiration. This work proposed a smart scheduling algorithm. However, it is only designed for a single fixed sensor.

For other existing related works, some of them revolve around IU classification methods [26–28], others focus on how to build a spectrum usage model [27, 29, 30], and some focus on how to predict future spectrum utilization [27, 31, 32].

Based on the above analysis, our work has improved the shortcomings of existing systems. Our system is the first crowdsourcing-based spectrum monitoring system with intelligent task scheduling algorithms. It is able to coordinate among mass mobile devices (e.g., smart phones with spectrum monitoring capability). Our system also requires IU pattern classification and prediction though it is not a focal point. Thus, we employ a common used classification method for IU pattern classification [33] and utilize a future pattern prediction method from [19].

2.2.2 System Model

Our system model consists of multiple IUs and a large group of SUs dispersed in a large geographical scale. All SUs are assumed to be mobile. As shown in Figure 2.2, the model shows that our SUs are controlled by a central controller. It coordinate SUs to detect the IU's occurrences.

There are two basic observations [19] that our system design follows: (I) IU signal has a semi-regular pattern. The spectrum usage pattern represents how IU behaves in the time and frequency domains. A particular distribution of the corresponding spectrum usage patterns can be found since the IU's activity is not completely random. A burst of IU transmission is

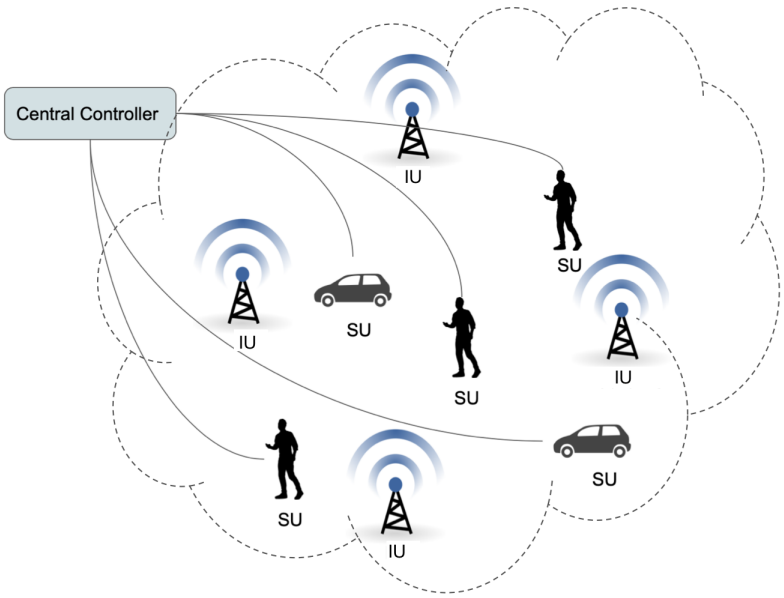

Figure 2.2: System Model

referred to as a IU occurrence, and the pattern of the IU is essentially a sequence in which its signal appears. Generally, the intervals between successive occurrences of a IU have an uneven distribution. (II) The pattern of IU occurrence is not completely fixed. We can learn about the occurrence of IU from the history. Moreover, we can also use the probability density function (PDF) of the IU pattern to calculate the probability of a IU appearing in a specific time period. Figure 2.3 shows the distributions of the occurrence intervals of four kinds of IUs from real spectrum monitoring trace. We can see that these distributions are approximately Gaussian distribution.

Since there already exist some distributed spectrum monitoring systems built on smart phones [20, 24], we can also assume all SUs in our system have spectrum monitoring capabilities.

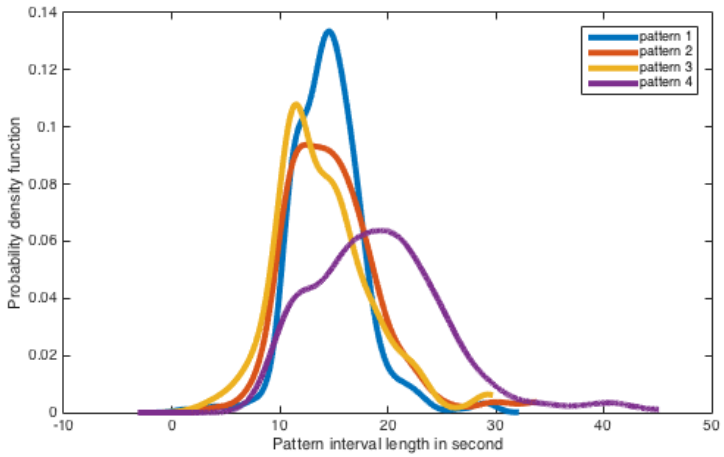

Figure 2.3: The PDF of the occurrence intervals τ of four different IUs from real spectrum monitoring trace.

2.2.3 Ideal Optimal Assignment

The core of our monitoring task is essentially the problem of coordinating SUs to achieve the optimal monitoring assignments based on IU occurrence time. In that case, we firstly propose the ideal optimal assignment. This step generates the optimal assignments under the condition that we know the exact IU occurrence time in the future and how much energy is left by other APPs. Its performance is considered as the upper bound for any other approaches.

Given a case where K IUs are dispersed on a certain area, and N SUs are moving inside this area. K IUs generate a total number of M occurrences within a certain period of time T. An occurrence is defined as a short period of consecutive transmission signal of IU. Denote T^k_{appear} as the appearance time of the kth occurrence and assume the indexes of the occurrences are sorted in ascending order of their occurrence time (i.e. $j < k \rightarrow T^j_{appear} < T^k_{appear}$). In our case, appearing time T_{appear} of each occurrence is given. The real-time location of N SUs are also known. For SU i ($i \in [1, N]$) and occurrence j ($j \in [1, M]$), define $A^j_i = 1(0)$ as

(not) assigning SU i to detect occurrence j. L_i^j denotes the relation of user i and occurrence j such that $L_i^j = 1(0)$ represents that user i is able (not able) to detect occurrence j. When monitoring the spectrum, SU devices require a short period of time to hop across different frequency bands, which is called a switching delay sd. A sensing duration dt is a small piece of time that SUs spend on capture an occurrence of IUs' behaviors. Monitoring power p_i is the power used when SU is active on spectrum monitoring.

Each SU has an energy budget E for spectrum monitoring. E_i^j shows the remaining energy of SU i at the appearance time of occurrence j. To calculate the value of energy budget E, we estimate an average energy consumption $aver\_E_i$ of all the other applications' usage, based on the real energy consumption $real\_E_i$ and charging times T_{charge} contained in a mobile usage database. The average energy consumption is calculated by total energy consumption between two consecutive charging time divided by the duration of time between two consecutive charging time. These three parameters are used for computing the SUs' available energy for spectrum monitoring.

The optimal existing IU monitoring problem is defined as: Given the above conditions, we want to optimally assign the SUs to monitor all of the IU occurrences while minimizing the total energy consumed by monitoring assignments. The optimization formulation assumes all monitoring needs will be successfully satisfied, which can be presented as Table 2.1:

Table 2.1: Minimize Energy Consumption

Situation 1:	Optimal formulation
Given:	L_i^j, E_i for $i \in [1, N]$, $j \in [1, M]$
	sd, T_{appear}, p_i, dt
Find:	A_i^j
Minimize:	$\sum_{j=1}^{M} \sum_{i=1}^{N} A_i^j \times dt \times p_i$
Subject to:	(2.1), (2.2), (2.3), (2.4)

There are four constraints for optimal formulation in situation 1. The first constraint cap-

tures the sensing range of each SU. Each SU only has a limit monitoring range. During assignments, SU i cannot be assigned for occurrence j if occurrence j is out of SU i's geographical sensing range, which can be formulated as:

$$if\ L_i^j = 0,\ A_i^j\ = 0,\ for\ i \in [1, N],\ j \in [1, M]. \tag{2.1}$$

The constraint above also reduces free variables in the problem.

The second constraint avoids assignment conflicts of a single user by assigning a user at most one time to the occurrences that appear within a period shorter than switching delay. That means one SU can only monitor one IU occurrence at a time by assigning an SU at most one time to the occurrences that appear within a period shorter than switching delay. This can be formulated as:

$$\begin{aligned} if\ j < k\ and\ T_{appear}^k - T_{appear}^j < sd + dt,\ then\ \sum_{j_1=j}^{k} A_i^{j_1} \leq 1, \\ for\ i \in [1, N],\ j,\ k \in [1, M] \end{aligned} \tag{2.2}$$

The third constraint prevents users for out of energy by ensuring that at any time. The energy consumption cannot exceed the amount of remaining energy of other APPs at energy budget, which can be expressed as:

$$\sum_{j=1}^{j_1} A_i^j \times p_i \times dt \leq E_i(T_{appear}^{j_1} + dt), for\ i \in [1, N],\ j_1 \in [1, M] \tag{2.3}$$

The forth constraint aims to ensure each occurrence can be detected at least by one sensor, as expressed as:

$$\sum_{i=1}^{N} A_i^j \geq 1, \ for \ j \in [1, M] \tag{2.4}$$

Sometimes due to the lack of SU devices or available energy for monitoring, the optimal formulation in Table 2.1 becomes infeasible. If this happens, the goal of optimal assignment changes into maximizing the sensing coverage, which means to detect as much occurrences as possible under the amount of energy budget. This can be formulated as another optimal problem in Table 2.2.

Table 2.2: Maximize Monitored Occurrences

Situation 2:	Infeasible Case
Given:	L_i^j, E_i for $i \in [1, N]$, $j \in [1, M]$
	sd, T_{appear}, p_i, dt
Find:	A_i^j
Maximize:	$\sum_{j=1}^{M} \sum_{i=1}^{N} A_i^j$
Subject to:	(2.1), (2.2), (2.3), (2.5)

The constraints for Situation 2 are the same to Situation 1 except for constraint 2.5. Under Situation 2, one occurrence can be detected by only one SU by no more than once. This can be formulated as:

$$\sum_{i=1}^{N} A_i^j \leq 1, \ for \ j \in [1, M] \tag{2.5}$$

The above two set of formulations should be repeated for each predesigned T.

It should be noted that both of the above situations (Situation 1 and Situation 2) require that the appearance time of each SU and the remaining energy of each SU be accurately known, which is obviously impractical. These two optimal assignment algorithms only provide an upper bound on the performance of SU assignment algorithm. Therefore, we propose greedy optimization method based on uncertain future for existing IU pattern monitoring

and heuristic assignments that approach optimal solutions.

2.2.4 Existing Spectrum Usage Pattern Detection

In previous study, We have proposed greedy optimization method and fast heuristic algorithm for existing spectrum usage pattern detection which are designed as practical alternative to the ideal optimal formulation.

Existing IU pattern monitoring leverages IU activity history in the spectrum databases for intelligent future spectrum monitoring. Firstly, we use a IU pattern classification to identify existing IU patterns and calculate the statistical distribution of occurrences in each pattern based on the similarity function [34].

For each existing pattern identified in the above process, we derive the statistical distribution of intervals between neighboring occurrences. Based on these distributions, two smart scheduling algorithms then assigns targeted monitoring tasks of existing IU patterns among SUs. Essentially, the existing IU pattern monitoring algorithm leverages the fact that efficient monitoring of known patterns does not need to monitor every frequency band all the time. It can perform targeted monitoring only on time and spectrum range where the patterns have a chance to occur.

Greedy optimization is designed to handle the uncertainty in the time and frequency information of IU occurrences and energy budget. The approach is to greedily allocate the energy-limited monitoring time so that we can maximize our statistical coverage of IU occurrences in a short period T_{step} from now (Figure 2.4). The coverage here is represented by the summation of probabilities of capturing the occurrences appeared within a T_{step}. Then we repeated at the beginning of every T_{step} as time progresses.

Since the greedy approach is a mixed integer programming problem, which is in general

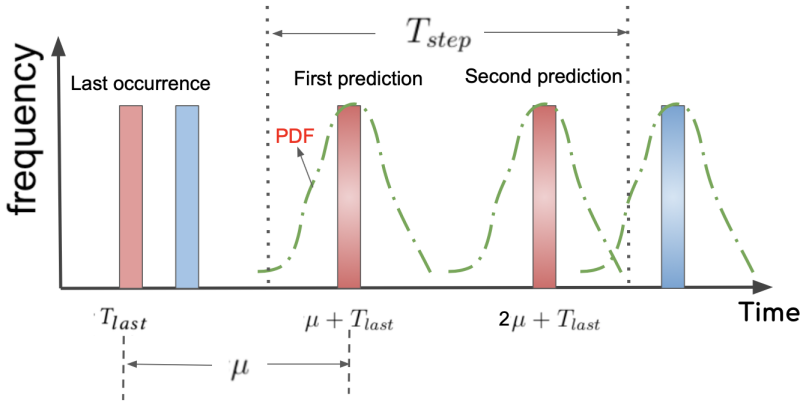

Figure 2.4: Future occurrences of the pattern after T_{last} can be computed as PDF function with its mean shifted to $k\mu + T_{last}$. Here, different color represents occurrences in different patterns.

NP complete. The fast heuristic algorithm is a substitute to directly solving the greedy optimization problem. In greedy optimization method, we use the optimization techniques to find the assignments that attain the largest coverage in the imminent T_{step} time, while in the heuristic algorithm, we design an iteration method to quickly generate the assignments with limited loss in coverage for this T_{step} time. There are 2 steps for heuristic approach. In step 1, we divide the PDF of a IU occurrence from the center into 7 sensing segments to identify segments as assignment units. Each segment has a length of a standard deviation σ of the PDF as shown in Figure 2.5. Step 2 is segment-based SU scheduling which is divided into two cases according to whether or not there exists any SU that is capable of monitoring the IU. Then we follow one of these two cases by judging which case will be encountered at the beginning of each T_{step}.

The algorithms presented above intelligently schedule the monitoring tasks for masses of portable mobile devices, by leveraging the existing IU occupancy patterns. In that way, we can reduce the energy consumption of IU monitoring.

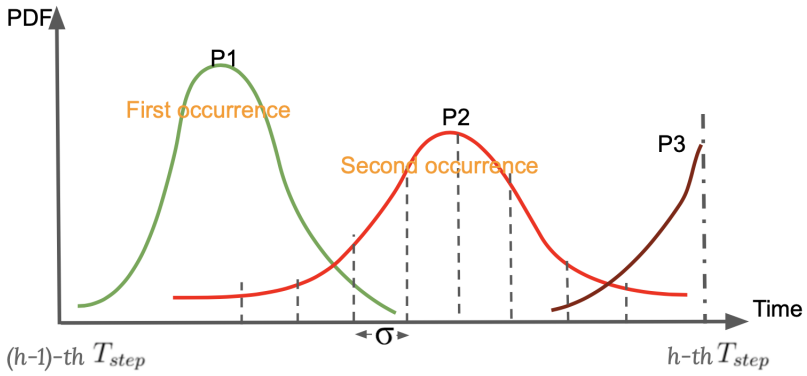

Figure 2.5: This figure shows how we divide the PDF into seven portions. The interval between two consecutive dash lines are a portion of σ.

2.3 Unknown Spectrum Usage Pattern Detection

2.3.1 Problem Statement

In previous works, we only authorize SUs to monitor the IU patterns that have occurred in the past. Nonetheless, as shown in [19], the definition of pattern exploration explained that the historical information we have might grow inaccurate as time goes by because of the IUs' spectrum access behavior change and mobility, which will finally degrade the performance of our proposed system. To keep our spectrum system updated with the dynamic spectrum, we also need to discover new IU pattern.

We use **unknown pattern** hereunder to represent new IU patterns that are not included in our existing pattern dataset. Our design aims to explore as many unknown patterns as possible while stably monitoring the occurrences of existing patterns. In this case, we suppose that after existing pattern detection at each T_{step}, SUs still have remaining energy and idle time to be utilized for exploring unknown IU occurrences

2.3.2 Optimal Assignment

Optimal assignment for the unknown IU pattern monitoring has the same formulations as those in existing IU pattern monitoring. We also can use Table 2.1 and 2.2 to generate it, except the occurrence i means unknown pattern occurrence. In this scenario, we assume an ideal situation where pattern occurrence sequence and the locations of all SUs and IUs are known beforehand.

2.3.3 Heuristic algorithm based on SU location

The optimization formulation is also impractical since the perfect circumstance in the consumption cannot be achieved. Therefore, we propose another heuristic task scheduling algorithm for unknown pattern detection. The core of this algorithm essentially lies in: (1) Without any prior information on new IUs, SUs randomly scan the spectrum to capture new IU occurrences. (2) If any new occurrences are detected, the central controller will quickly model the the distribution of new occurrences intervals, which will be used for occurrence prediction afterwards. This procedure will make our exploration on new IU patterns be more targeted and accurate.

The heuristic scheduling algorithm will be described into five parts: SU groups generation based on locations, SUs monitoring schedule, random monitoring, target monitoring and update patterns in existing pattern sets.

1. **SU groups generation based on locations**

   In our case, we assume the sensing range of a device and the broadcast range of a incumbent transmitter are both circular. All SU devices are supposed to have the same sensing range. Intuitively, different SUs will have high correlation in sensing

outputs if they are geographically close enough to each other. We define the devices whose sensing ranges have adequate overlap as one group. As shown in Fig 2.6, we show a possible distribution of 4 SUs. SU 1,3 and 4 are fairly close to each other thus compose a group; SU 2 also gain adequate overlap with SU 1 thus form another group. We treat the SUs in a group as an aggregate while assigning sensing tasks to reduce energy consumption for each SU.

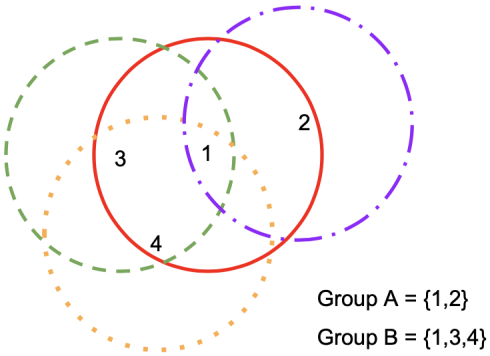

Figure 2.6: An example of 4 users forming 2 groups

Here comes a trade-off between energy consumption and sensing accuracy when choosing the value of overlap. On one hand, smaller overlap may result in a loss of sensing accuracy since a SUin that grid may have higher probability not being able to detect the same signal as another SU.On the other hand, the number of SUs in a grid decreases as the overlap increases, which means a SU contributes more energy to form a grid. In this paper, all SU devices are supposed to have the same sensing range, hence we set the overlap to 80% of a devices sensing range. This value is adjustable in different cases.

2. **SUs monitoring schedule**

For each group, we need to decide how to monitor SUs that inside it to maximize the

aggregated monitoring time. There are two problems that we need to solve: (1) How much usable time will this group have? (2) How much time and energy each SU should contribute to this group? For each T_{step}, the assignable time of a group is determined by the idle time and energy of the SUs inside it. Our goal is to assure as much usable time as possible for that group. Therefore, we set a metric $R_{user\_in\_group}$ as the criterion to allocate SUs' idle periods to the groups. That means, the larger $R_{user\_in\_group}$ value a SU has, the more valuable it has to its group compared to other SUs. This metric is determined by the sensor priority Sp and remaining energy E_i of SU i as:

$$R_{user\_in\_group} = Sp_i \times E_i \tag{2.6}$$

Where **sensor priority** Sp is a parameter characterizing the importance of a SU's monitoring service in a group, which is related to the number of SUs in that group. If a group contains many SUs, it is trivial not assigning a particular SU to sense an occurrence since it is easy to find alternative SUs for that monitoring task. That means, the priority of SUs in group A is computed as the reciprocal of group A's user number. If a SU is included in multiple groups (shown in Figure 2.6), it will be treated as different devices as in computing the corresponding metrics. For example, if SU 1 is in both group A and B, suppose group A and B has 2 and 3 SUs respectively, the rewards of SU 1 in group A and B are calculated as:

$$\begin{aligned} R_{1\_in\_A} &= \frac{1}{2} \times E_1 \\ R_{1\_in\_B} &= \frac{1}{3} \times E_1 \end{aligned} \tag{2.7}$$

In each step, all the values of $R_{user\_in\_group}$ are sorted in a descending order. Then, we allocate the idle time of each SU to its corresponding group following this list of

$R_{user\_in\_group}$. Specifically, when taking an entry of $R_{i\_in\_A}$ in the list, we first check if T_{step} is totally covered in group A. If the answer is yes, we skip to check the next entry in the list. Otherwise, we allocate SU i's idle time for monitoring job in group A. The process continues until T_{step} is totally covered in every group or no usable time or energy of the SUs is left. Time segments of different SUs assigned to the same group should not be superposed as to reduce energy consumption.

3. **Random Monitoring**

   The coordination method can help groups to jointly sense a segment. It can be divided into two stages, first is random detection stage and second is targeted detection stage. Random detection is executed before any unknown pattern occurrence is found. Targeted detection is executed after the models of newly detected unknown patterns are built.

   During first several T_{step}s, since no prior knowledge on where and when a new pattern will appear is given, we uniformly divide the groups' sensing time into multiple small pieces and randomly select a frequency band to sense during each time piece. If any unknown occurrences are found, we record the time and frequency of those occurrences, and the locations where the SUs stayed when detecting the new patterns. We also cluster the occurrences into different patterns. This stage creates the unknown pattern dataset.

4. **Targeted Monitoring**

   After capturing at least one new pattern, we can enter the targeted detection stage. Given the newly discovered IU patterns, we compute the mean and deviation of each patterns intervals to model its statistic distribution. In the preliminary phase, it's more likely that we do not have sufficient samples to accurately characterize the new patterns.

We can see from the observations in Figure 2.3 that the distributions of different pattern intervals are approximate Gaussian distributions. Therefore, when pattern samples are inadequate, we model the pattern intervals as Gaussian distributions using computed mean and deviation. If only two occurrences of a pattern are found, we use the interval between these two occurrences as the mean value, and choose the average deviation of all kinds of patterns within the dataset as the new pattern's predetermined deviation. If just one occurrence of a pattern is detected, we use both the average mean and deviation of all kinds of patterns as the preset values for modeling. The mean and deviation value will be updated after each T_{step}.

We will be able to use the rough pattern interval models to predict where and when other new occurrences of this IU pattern will appear in the next T_{step}. The heuristic approach in existing IU pattern monitoring then adopted here to generate a group's sensing scheduling, except that the "worker" is changed from a single SU to a group. Firstly, we also need to divided the PDF of the newly discovered IU patterns into 7 *sensing segments*. and each segment has a length of a standard deviation σ of the PDF as shown in Figure 2.5. Assuming that IU occurrences follow a PDF similar to normal distribution, which has been validated in analysis of IU behaviors as shown in Figure 2.3, the probability that an occurrence appears outside of the 7σ range can be approximated as 0. Each segment is the smallest time unit considered in our scheduling algorithm. Given the energy that should be reserved for each group at each T_{step}, the goal of our scheduling algorithm is to properly utilize the energy within each T_{step} to monitor as much segments as possible for all pattern occurrences in T_{step}. If each segment of every occurrence has an assigned group to monitor the corresponding IU's activity, then all IU activities will almost surely be captured.

Secondly, there are **two cases** for task scheduling in each segment: (1) The monitoring

task of a segment will be assigned to only one group if there exists one or more groups that have adequate time to monitor the IU over the entire segment. (2) If no group can cover the whole segment, the segment is divided into even smaller pieces so that multiple groups, each covering some of these pieces, can coordinate to monitor the segment.

For both cases, we record the start and end time of each segment, and calculate its corresponding CDF $prob_j^k$ based on the approximate distribution. L_i^j is the relation between an pattern j and a group i. Based on L_i^j, we then obtain a list of groups that are able to sense a particular segment. Next step is to check within this list to find the groups that have adequate time for covering the desired segment. If such group exists, we have **case 1**. We calculate the *reward* for those groups using function 2.8. Group with the largest *reward* will be selected to sense the entire segment. Specifically, $reward_{i,j}^k$ is designed to be a product of three factors as follows:

$$reward_{i,j}^k = w_{i,j}^k \times E_i \times priority_i^j, \tag{2.8}$$

Where $w_{i,j}^k$ denotes the group i's relative profit of sensing the segment k of IU j's occurrence comparing to the choices of monitoring the segments of other IUs' occurrences, E_i denotes the remaining energy of group i, and the $priority_i^j$ denotes denotes how valuable is group i's potential monitoring service for occurrence j comparing to the other possible choices of groups for this monitoring job.

The calculation for energy budget E_i follows:

$$E_i(t) = \frac{E_{battery}^i(t) - E_{app}^i(t)}{total\ number\ of\ T_{step}s\ before\ T_{charge}^i}, \tag{2.9}$$

It is based on the profiles of mobile device usage. Using the usage information, at the

current time t, we can predict the time when the next charging event will happen, denoted as T_{charge} , and other applications' future energy consumption till the next charging event , denoted as $E_{app}(t)$. We can also obtain the current battery energy $E_{battery}(t)$.

$w_{i,j}^k$ can be expressed as:

$$\begin{aligned} & w_{i,j}^k = prob_j^k \times L_i^j \\ & if\ w_{i,j}^k > 0 \\ & \quad w_{i,j}^k = w_{i,j}^k - maxw_j^k \\ & end \end{aligned} \tag{2.10}$$

Where $prob_j^k$ is the probability that an IU j's occurrence appears in segment k, which is calculated by:

$$prob_j^k = CDF\left(SensingEnd_j^k - SensingStart_j^k\right) \tag{2.11}$$

where $SensingStart_j^k$ and $SensingEnd_j^k$ represent the start and end point of the corresponding segment.

$maxw_j^k$ is the largest w value that can be obtained by group i if group i spends segment k's time to monitor other IUs occurrences instead of IU j's occurrence, which can be expressed as:

$$maxw_j^k = \max_{l \neq j,m} w_{i,l}^m L_i^l O_{j,l}^{k,m}, \forall i, j \text{ satisfying } L_i^j = 1, \tag{2.12}$$

where $O_{j,l}^{k,m} = 1$ if segment k of IU j's occurrence time overlaps with segment m of IU l's occurrence time and $O_{j,l}^{k,m} = 0$ for other cases. Essentially $maxW_j^k$ is a loss that should be taken into account for relative profit calculation because a group cannot simultaneously monitor multiple IUs' signal. If a group is allocated to monitor a

segment of one IU, it will lose the probability of capturing occurrences of other IUs.

For the $priority_i^j$, assume a group i is able to hear more than one IUs' signal, the urgency of mandating group i to monitor a particular IU j's segment is related to the number of groups within the area that can also sense IU j's signal. If many groups can detect IU j's signal, then it is not a big issue to arrange group i to sense other IUs' signal since it is easy to find alternative groups for the monitoring task of IU j. Thus, the $priority_i^j$ will be small in this case. Based on this reasoning, we define

$$priority_i^j = 1 - \frac{X_j}{\sum_{l \in G(i)} X_l} \tag{2.13}$$

where X_j denotes the number of groups that can capture IU j's occurrence and $G(i)$ is defined as the set of IU that can be detected by group i.

Similarly, **case 2** happens when we cannot find any group in the list having enough idle time to cover the entire segment. Under this case, we divide the segment into even smaller time chips and assign the chips to available groups following the same rules as allocating entire segments to the groups. The group with the largest value of *reward* will offer its best effort to cover as much of the segment as it can, and leave the remaining segment to the group with the second largest *reward* and so forth, until the segment is completely covered or no group is available for the assignments. Since a time chip is much smaller than a segment, it is easy to find a group with adequate energy to cover the chip.

For each segment, we determine which case it will run into and then perform the steps above.

After groups scheduling is finished, we uniformly divide the remaining sensing time of each group and randomly choose a frequency band to detect unknown patterns, which

is the same as in random detection stage.

5. **Update patterns in existing pattern sets**

   At the end of each T_{step}, we have three updates in existing pattern sets. On the one hand, if during a certain period of time, an unknown IU pattern is stably detected, which means its location information and the mean and deviation of its interval distribution do not change much, this pattern can be added into the existing pattern dataset. We will also cluster the detected new pattern occurrences and update the mean and deviation value of each pattern interval distribution. New location information is also recorded. On the other hand, after a certain period of time, a IU pattern that cannot be detected any more will be removed from our dataset.

2.4 Experiment

During our experimental process, we use the real world data for simulation to evaluate the performance of our spectrum monitoring system. We used the ideal optimal assignment as a higher bound and the random detection method as a lower bound.

There are 44 types of real IU patterns that extracted from CityScape Observatory spectrum database [2] in our case. 34 of them are presented from the beginning of an simulation as the existing IU patterns. Another 10 of them are used as unknown IU patterns which start in the middle of the simulation. In Figure 2.1, we can see 4 examples of IU patterns.

In our experiment, taxi trajectories are used to represent the movements of 100 SUs. We utilize the mobility traces dataset of taxi cabs in San Francisco [35] that contains the GPS coordinates to represent SU mobility traces. Figure 2.7 shows a smaller scale of our simulation setting with 60 taxi traces and 10 IU deployments.

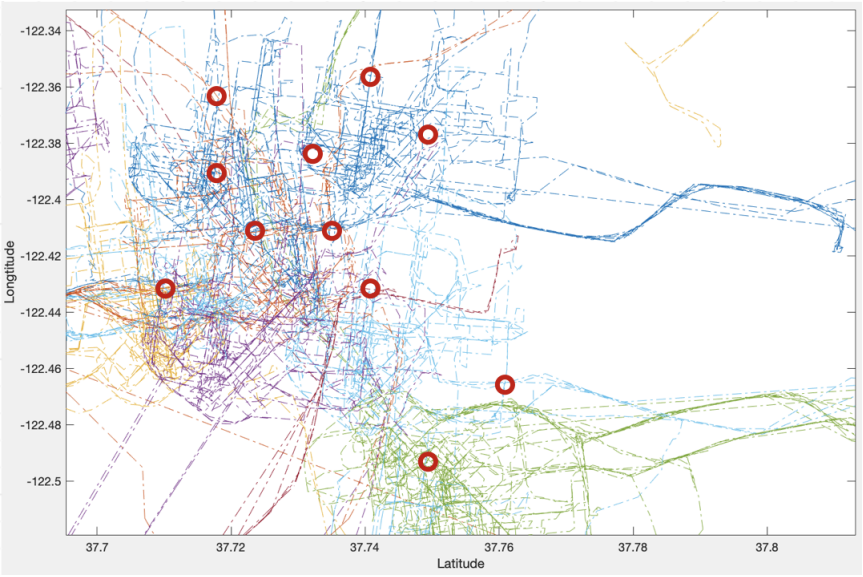

Figure 2.7: A smaller scale illustration of SU mobility simulation (circles: IU, dash-dot lines: taxi movement trajectories)

In order to determine how much energy a SU can spare on spectrum monitoring and ensure our evaluation is based on real energy consumption on mobile device, we utilized a Device Analyzer dataset from University of Cambridge [36] which contains: (1) times when a phone is turned on and off; (2) times at which the phone is charging; (3)real time battery level and voltage, etc. Therefore, we are able to compute real energy consumption of phone applications which can be used for computing 2.9. According to [20], SU devices being active on sensing draws about 1.5W as the monitoring power. For computing the energy consumption of optimal assignments, we set sensing duration dt as 5ms based on [19] and the frequency switching delay in our simulation to 50ms [20].

In existing IU pattern monitoring experiment, we simulated a crowdsourcing spectrum monitoring scenario, in which 34 IUs transmitting known patterns are deployed among 10 to 100 SU traces (traces of taxis). One T_{step} lasts for 5 seconds. At each T_{step}, SUs report their locations to the central controller. We use the practical data over 2 hours for performance evaluation.

We compared the existing pattern coverage among the two existing IU pattern monitoring algorithms and our benchmark. The results showed that as the number of SU increases, the coverage increases significantly. The performance of the greedy optimization method is slightly better than the heuristic algorithm because the heuristic algorithm does not really guarantee the optimal solution. We also tested energy consumption evaluation and the number of SU available for spectrum monitoring changes over time. From the total energy consumption, we can conclude that as the number of SUs increases, more total energy is used to better cover the IU signals. As more sensors share monitoring, the energy consumption of per SU actually decreases. The number of SU available result indicate that the available user ratio of benchmark always stays 1, and the ratio of two proposed methods are fluctuating below 1. Since we update users energy after each T_{step}, we do not observe a large decrease in available user numbers of two proposed methods.

2.4.1 Unknown IU Pattern Monitoring

For the simulation of unknown IU pattern monitoring, we add 10 more unknown patterns besides the 34 existing pattern. Unknown pattern detection is executed right after known pattern detection within each T_{step}, therefore uses the identical sensor parameters, mobile data and trajectories over 2 hours. However, in this part of simulation, we assume that no pattern type or occurrence time or location is known beforehand. **Successfully detect an occurrence** is defined as: (1) frequency band of an occurrence is within the detection frequency band; (2) appearing time of an occurrence is within the detection time frame; (3) the device used for detecting an occurrence is under the geographical coverage of the occurrence's corresponding IU.

As a reference, we run a random detection algorithm. That is, under identical circumstances (i.e., identical distribution of secondary devices and IUs, identical secondary device usages,

identical group components), the available sensing time of each SU is uniformly divided into small time chunks with 50 ms in length. We use each time segment to randomly monitor a frequency band, as the first several steps that we described in Section 2.3. Different from our proposed algorithm, this random detection method is not able to learn from history.

First, we compared the unknown pattern coverage between SU location based heuristic algorithm, the random detection method and our benchmark, which represents their capability of exploring new patterns. This unknown pattern coverage is defined as:

$$UP\ coverage = \frac{DetectedUnknownPatternNumber}{TotalUnknownPatternNumber} \tag{2.14}$$

As in Figure 2.8, along x-axis, we also increase the SU number from 10 to 100 to see the changes in performance. The output of random detection method is barely 25% percent of the output of our method. This is because our method has learning ability, which random detection method does not maintain. Our method can extract useful information from history, therefore each assignment it makes will have a tendency towards the possible repeated patterns such that the coverage is greatly improved. There is still a gap between our method and ideal optimal assignment (Benchmark). Benchmark is computed under perfect condition (i.e. all information of SUs and IU patterns is known beforehand), while our method assumes no prior information can be obtained. The performance of our method is also affected by running time. With shorter running time, the system can only build rougher pattern interval model; while with longer running time, the system can acquire longer learning period and generate more accurate pattern models for scheduling.

Since our unknown pattern detection is executed after existing pattern detection at each T_{step}, more energy will be consumed per T_{step}. A concern is whether this unknown pattern detection will impose bad effect on existing systems performance and stability; if it does,

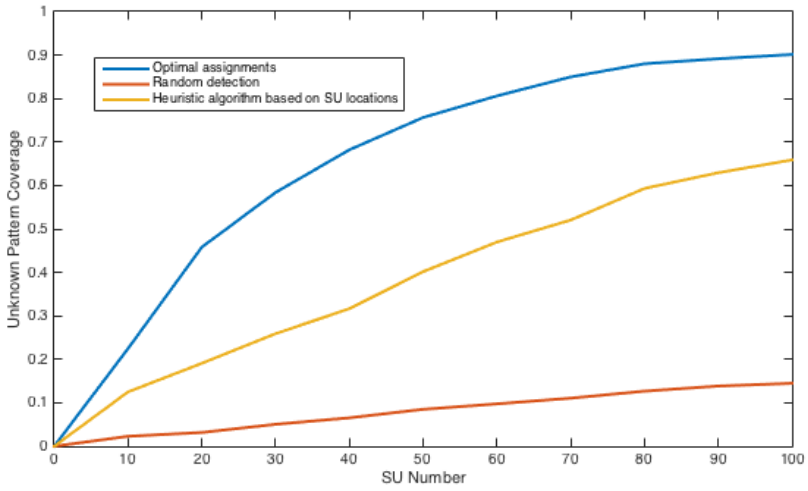

Figure 2.8: Unknown pattern coverage comparison. (Blue line: ideal optimal assignment. Yellow line: Proposed method. Red line: Random detection)

how large the effect will be. Figure 2.9 presents the existing pattern coverage of optimal assignments as well as heuristic algorithm with and without unknown pattern detection. There is indeed a coverage drop after adding unknown pattern detection. However, this drop decreases as the pattern-user ratio decreases. This ratio is defined by:

$$IU\ ratio = \frac{OptimalAssignments}{UserNumber} \tag{2.15}$$

which represents the average sensing tasks each SU is responsible for. Intuitively, the average life time of the SUs will be increased if they are used less for average. It will reduce the cases where the SU's battery dies while the system is running. We believe that a small drop in existing pattern coverage is worthy of exploring more unknown patterns in the dynamic spectrum.

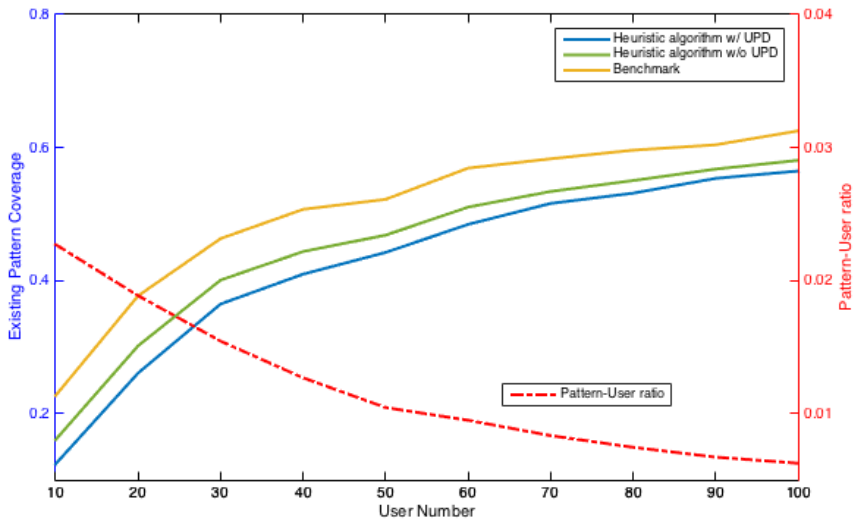

Figure 2.9: A comparison showing how the unknown pattern detection (UPD) affects existing pattern coverage. The left side shows the existing pattern coverage. Benchmark, heuristic algorithm without UPD and heuristic algorithm with UPD are presented using a yellow, green and blue line, respectively. The right side shows a pattern-user ratio in red dash-dot line that tells average sensing tasks each user is responsible for.

2.5 Conclusion

In this chapter, we described our novel crowdsourcing-based spectrum monitoring system at a large geographical scale which intelligently schedule the monitoring tasks for masses of portable mobile devices, by leveraging the IU occupancy patterns. The previous existing IU pattern monitoring algorithms discovers the dynamic patterns of past spectrum activities to improve monitoring efficiency and reduce energy consumption.

In order to discover unknown IU patterns that are not included in our existing pattern dateaset, we proposed the unknown IU pattern monitoring heuristic algorithms based on the location of SUs. The simulation results show that our system achieves a high spectrum monitoring coverage and does not require any additional infrastructure. With the unknown IU pattern detection scheme, the ability starting with zero knowledge of the past, makes our

system capable of running efficiently not only on the existing spectrum utilization databases but also on the situation where no historical spectrum information is accessible. It gradually create the pattern dataset and improve its monitoring intelligence based on the past data. New pattern exploration is not isolated from our scheduling algorithm. The scheduling algorithm always uses up-to-date spectrum information obtained from both existing and unknown monitoring algorithms, thus is not wedded to a wrapped dataset.

Chapter 3

Energy Harvesting-based Spectrum Monitoring System

3.1 Introduction

3.1.1 Motivation

In Chapter 2, we design the spectrum monitoring system which is powered by batteries (Figure 2.2). However, the system frequent scanning the spectrum, which is traditionally powered by batteries, burdens the energy conservation [11]. This raises a non-trivial problem regarding the system lifetime. A system composed of a large number of spectrum sensors may take several days or months to complete the specified sensing task. As time proceeds, the battery power in a sensor will be exhausted and the sensor will shut down. Additional manpower is needed to reactivate the dead sensor. To alleviate such problems, one may consider the use of energy-harvesting to power the sensors [37–39]. Energy harvesting refers to the removal of energy or the conversion of energy from one form to another. When it

is applied to a sensor node, energy from an external source can be collected to power the node to increase its life and capacity [39]. Solar power, though uncontrollable, is one of the most commonly selected energy for harvesting because of its predictability with daily and seasonal pattern. Therefore, we consider to utilize the solar energy to power our spectrum monitoring system.

3.1.2 Contribution

In this chapter we propose a solar energy harvesting-based energy management scheme to support our spectrum monitoring system over a large geographical area. Compared with our previous system, this energy harvesting-based spectrum monitoring system changed its power supply mode to solar energy. We proposed a Long short-term memory recurrent neural network which can accurately predicts incoming solar power. We also proposed a solar power management scheme, which makes the system work continuously during both day and night time without running out of power and intelligently utilize the predicted solar energy to carry out monitoring tasks. Comparing our proposed LSTM deep RNN network with general RNN and notwork with no Tanh and Sigmoid layers, the evaluation results shows our new design greatly outperforms the existing prediction networks. We also evaluate the performance of energy harvesting-based spectrum monitoring system compared with battery-based system which indicates our scheme supports continuous operation of our previous spectrum monitoring system using harvested energy and make our system a stable and efficient spectrum detection system with multiple low cost sensors.

3.2 System Model

As shown in Figure 3.1, Our system model consists of multiple IUs and sensors dispersed in a large geographical scale which is basically the same as previous model in Figure 2.2. Compared with battery-based system, we changed all spectrum sensors to static and solar-powered[39] sensors from the mobile SUs. Sensors are controlled by a central controller. The design of this model is also based on two basic observations which are the same as in 2.2.2.

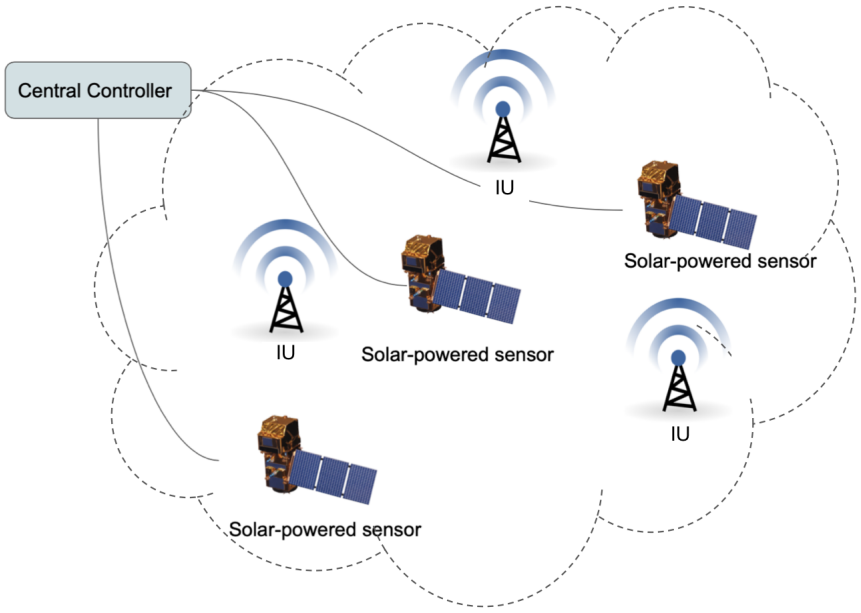

Figure 3.1: System model of our energy harvesting-based spectrum monitoring system

3.3 Ideal Optimal Assignment

In this section, we formulate the problem that needs to be solved into an optimization problem. The formulations are basically the same as our previous optimal formulations (Section 2.2.3) except for the SUs are stable solar sensors and energy constrains.

As we discussed before, we also given a case where K IUs and N sensors are randomly placed on a certain area, the sensors' location and IUs' broadcast range are already known. Within a certain period of time T, K IUs generate a total number of M occurrences, where each occurrence is a small piece of consecutive transmission signal from an IU. For sensor i ($i \in [1, N]$) and occurrence j ($j \in [1, M]$), $A_i^j = 1(0)$ is defined as (not) assigning sensor i to detect occurrence j. Relation of sensor i and occurrence j is represented by L_i^j, where $L_i^j = 1(0)$ denotes that sensor i is (not) able to detect the radio signal of occurrence j.

During spectrum monitoring, a short period of time called a switching delay sd is required by a sensor to switch among different frequency bands. Each sensor spends a sensing duration dt to capture the behavior of the IU. We use p to denote the monitoring power when sensor is active on spectrum monitoring.

The solar power harvested by sensor i between occurrence $j-1$ and occurrence j is denoted as Ps_i^j. Each sensor's available energy at the beginning is B_0. The maximum capacity of backup battery where the harvested energy is stored is B. ξ is the conversion efficiency showing how much the incoming solar power is converted into electric power. There will also be a power leakage P_{leak} when the sensor is running.

With the above assumptions, our goal is also to satisfy all monitoring needs by optimally assigning the sensors to capture every IU occurrence, meanwhile minimizing the total energy consumed by the monitoring tasks. We present the optimal formulation as Table 2.1. For the constrains in this table, (2.1) (2.2) and (2.4) are the same as which in Section 2.2.3. The only difference is the "SUs" are changed to "solar sensors" instead. The third constraint (2.3) meets the requirement of energy neutral operation which ensures that sensor never dies due to energy exhaustion [39]. At any time, the remaining energy of the backup battery can neither exceed its maximum capacity nor be less than zero, which can be expressed as:

$$B \geq B_0 + \sum_{j_1=1}^{k} [\xi P s_i^{j_1} - A_i^{j_1} \times dt \times p_i - P_{leak} i] \geq 0, \quad for\ i \in [1, N],\ j_1 \in [1, M] \tag{3.1}$$

In some cases, the above optimal formulation is infeasible due to the lack of sensors at certain areas or the lack of energy at some sensors as the same as situation 2 in Section 2.2.3. For these cases, we reformulate our goal to maximize sensing coverage, meaning that as many occurrences as possible should be detected under the energy budget. This formulation is shown in Table 2.2. The constraints (2.1) (2.2) and (2.5) are the same while the (2.3) is replaced by constraint (3.1).

3.4 Heuristic Algorithm

The optimal assignment problems formulated in Section 3.3 cannot be realized. They are only the upper bound on the performance of sensor assignment algorithm because they need prior knowledge of incoming solar power, and appearance time and frequency of spectrum occurrences. Such information cannot be obtained beforehand due to the stochastic nature of solar power and spectrum occurrences. Therefore, we changed the energy management scheme in the heuristic algorithm to make our energy harvesting-based spectrum monitoring system approaches to optimal solutions.

Essentially, the heuristic algorithm is a way to achieve optimization results through an iterative approach. To attain accurate heuristic assignments, we must solve two problems in the optimal formulation: 1. How to accurately predict future incoming solar power? 2. How to intelligently utilize the solar energy to carry out monitoring tasks? We divide the heuristic algorithm into two parts. The first part describes how we predict the incoming

energy accurately, and the second part presents our smart scheduling algorithm and power management within the system.

3.4.1 Incoming Solar Energy Prediction

Due to the high availability and low cost, solar energy is used to provide sustainable energy to our spectrum sensing system. Since generation of solar energy depends on weather and meteorological parameters, a strong power management algorithm with energy forecasting is required to ensure uninterrupted operation of the spectrum sensing system. If there is no accurate energy prediction, any unexpected energy changes in incoming solar energy can severely affect the system's daily operations and even lead to system outage.

Studies on solar power prediction in energy harvesting can be classified as: machine learning algorithms, physical techniques [40–42] and combination of the above two[43, 44]. Among them, the learning techniques proposed in [43, 45] show the best prediction accuracy on solar power. Specifically, the long short-term memory recurrent neural network (LSTM-RNN) based approach used in [43] has high performance while in [45] the deep RNN achieves low error rate. In this work, we combine these two techniques to leverage both of their benefits.

Conventional RNNs remembers things for just small duration of time, it can solve sequence handling to a great extent but not completely. LSTM-RNN is designed to model the temporal data sequences and their long-term dependencies, whose capability outranges the conventional RNNs[46]. However, prediction of one layer LSTM-RNN is still inaccurate. Based on the reasons above, our LSTM-RNN model is designed to have three hidden layers plus an input and output layer, as shown in Figure 3.2. This network includes a LSTM-RNN layer to greatly boost performance, and a nonlinear hyperbolic tangent layer and a sigmoid layer to reduce the error rate. We adopt Xavier-He initialization[47] for selecting an desirable

initial weights of the network. *ADAM* optimizer with 20% dropout rate is implemented for regularization[48]. 10-fold cross validation was utilized to confirm of stability of predicted result. The batch size is set to 16. A mean-absolute loss function is used to train the network. Evaluation results based on real world data (see section 3.5) shows that our new design greatly outperforms the existing prediction algorithms.

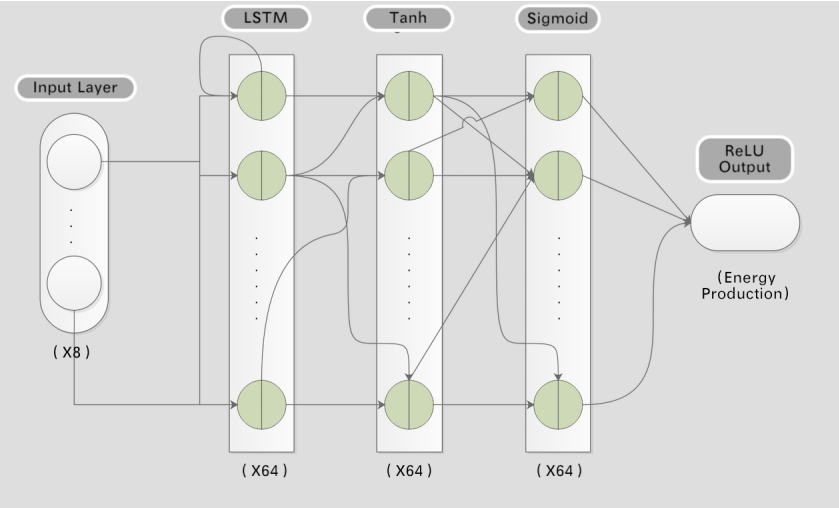

Figure 3.2: Depiction of the architecture proposed LSTM-RNN. The LSTM layer greatly improves network performance. The nonlinear hyperbolic tangent and sigmoid layers exhibit lower errors than the standard linear activation function.

3.4.2 Monitoring Task Scheduling

Given the solar power prediction algorithm in the previous section, in this subsection, we discuss our intelligent monitoring task scheduling algorithm. The task scheduling algorithm takes four steps which are almost similar to the previous algorithm (see Section 2.3.3) except the energy budget part and the workers change from "SUs" to "solar sensors". In step one, we divide the entire sensing period T into multiple periods of size T_{step}. Then, in step two, we compute the energy that a sensor can spent for IU detection in each T_{step}. In step three, for each T_{step}, we compute the distribution of a IU's occurrence appearance time. Finally,

we decide how to dispatch sensors to detect that occurrence based on the appearance time distribution, sensor availability information and available energy budget. Hence, in the following, we describe the details of step two and three.

Energy Budget for each T_{step}

With the LSTM-RNN model in Section 3.4.1, we can predict the incoming solar power Ps_i^t of sensor i at time t within each T_{step}. To ensure that the system can function normally during the night when solar power is not available, a power management scheme is used to save a certain portion (denoted as r_night) of harvested power at daytime into the battery. This reserved power, denoted as $reserved_i^t$, can be expressed as: $reserved_i^t = r\_night \times Ps_i^t$. The total usable energy E_i^t for each sensor i at a daytime time t within T_{step} is:

$$E_i^t = Ps_i^t - reserved_i^t. \tag{3.2}$$

For a particular sensor s_1, its reservation ratio r_night is computed by:

$$r\_night(s_1) = \sum_{i=1}^{m} \lambda_i \times \eta_i, \tag{3.3}$$

where m is the number of IUs that s_1 can detect. r_night is determined by two factors: night pattern ratio λ and sensor number ratio η. λ_i shows the percentage of pattern i's occurrences that appear at night time out of all the occurrences within 24 hours, which can be expressed as:

$$\lambda_i = \frac{number\ of\ pattern\ i\ occurrences\ during\ the\ night}{total\ number\ of\ pattern\ i\ occurrences} \tag{3.4}$$

The η_i in (3.3) represents the urgency of demanding this particular sensor s_1 to detect pattern

i, which can be formulated as:

$$\eta_i = \frac{n_i}{\sum_{l=1}^{m} n_l} \tag{3.5}$$

Here n_i is computed by

$$n_i = \frac{total\ number\ of\ pattern\ i\ occurrences}{number\ of\ sensors\ that\ can\ detect\ pattern\ i}. \tag{3.6}$$

Essentially, n_i captures the average responsibility of detecting pattern i considering all sensors that can capture the pattern i.

Distribution of occurrence time

For the following steps, they are almost similar as we show in Section 2.3.3. As shown in Figure 2.1, different IU has different occurrence pattern. From spectrum monitoring history data, we can learn the distribution of the occurrence interval of each IU pattern, which then can be used to predict when occurrences appear within T_{step}. After we extract IU patterns using the methods in section 2.2.4, we treat each pattern identified by this method as the transmission from a IU. Next, we focus on analyzing an individual pattern. Define the time between two consecutive occurrences in the same pattern as the pattern interval τ. The statistical distribution of τ can be computed based on this pattern's historical data as shown by the PDF function in Figure 2.5. Its mean μ determines the mean occurrence interval, and standard deviation σ measures the variation of occurrences in each pattern. Assuming T_{last} is the last time where we observed an occurrence of a IU pattern, the distribution of the k_{th} future occurrence of the pattern after T_{last} can be computed as the PDF function in Figure 2.4 with the mean shifted to $k\mu + T_{last}$.

Sensing Segment

Note that previously, we have divided the entire sensing time period T into smaller time steps with length T_{step}. As shown in Figure 2.4, we further divide the PDF of a pattern's occurrence time into 7 segments of length σ and assume that the probability that an occurrence appears outside of the 7σ range can be approximated as 0. Each segment is the smallest time unit considered in our sensing scheduling algorithm. Given the energy that should be reserved for each sensor at each T_{step}, the goal of our sensor scheduling algorithm is to properly utilize the energy within each T_{step} to monitoring as much segments as possible for all pattern occurrences in T_{step}. If each segment of every occurrence has an assigned sensor to monitor the corresponding IU's activity, then all IU activities will almost surely be captured by our sensor scheduling algorithm. Next, we divided our algorithms into two scheduling cases based on whether there exists a sensor that has adequate energy to monitor the IU for the entire sensing segment which is the same as we discussed in section 2.3.3.

3.5 Experiment

In our experiment, we assume all sensors are static. 100 sensors are randomly distributed in the broadcast range of 10 IUs. These sensors are working together as a spectrum monitoring system. We set the experiment time to be two hours, with one hour before the sunset and one hour after it. We evaluate the performance of our heuristic scheduling algorithm with the optimal assignments as a performance upper bound and a battery based scheduling algorithm as a comparison.

LSTM-RNN performance evaluation

To train our LSTM-RNN, we use the sensor data of 100 different locations in the National Centers for Environmental Information(NCEI) database as the training and testing dataset. NCEI database provides public access to the Nation's treasure of climate and historical weather data and information measured every five minutes including air temperature, precipitation, solar radiation, surface temperature, etc[49, 50]. Solar radiation is treated as labels in our network. Training dataset contains the data from June 1st to 20th 2018, and testing dataset contains the data from June 21th to 30th. Once the network is trained, we will be able to predict the average incoming solar radiation $Rm(i)$ of 100 sensors from June 21th to 30th in every five minutes. Figure 3.3 shows the training mean-absolute-error (MAE) comparison among our LSTM-RNN network, Conventional RNN and one layer LSTM-RNN during 100 epochs. Figure 3.4 presents our test MAE among three networks above. The results indicate our network outperforms the other networks. Figure 3.5 shows parts of our results on incoming solar power prediction. We obtained fairly good prediction using the proposed LSTM-RNN. Thus, predicted harvested energy for each T_{step} equals to $Ps_i^t = \frac{Rm(i)}{60} \times panelSize \times \xi$. $panelSize$ is the size of solar panel equipped with every sensor in our simulation, and is defined as 1 m^2. ξ denotes the conversion efficiency from energy generator to energy storage which is set to be 85% [51].

Solar energy harvesting system evaluation

In the following, we will evaluate the performance of our energy prediction and mangement scheme by showing comparison results between battery-based spectrum monitoring system and solar energy-harvesting based system.

Firstly, to demonstrate that the solar panel size used in our simulation system is reasonable,

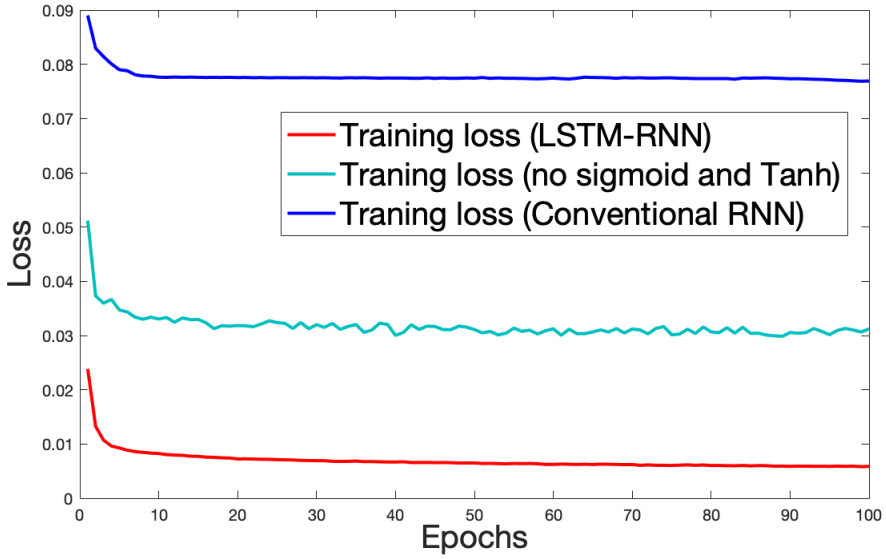

Figure 3.3: Training mean-absolute-error (MAE) comparison among our LSTM-RNN network, Conventional RNN and one layer LSTM-RNN during 100 epochs

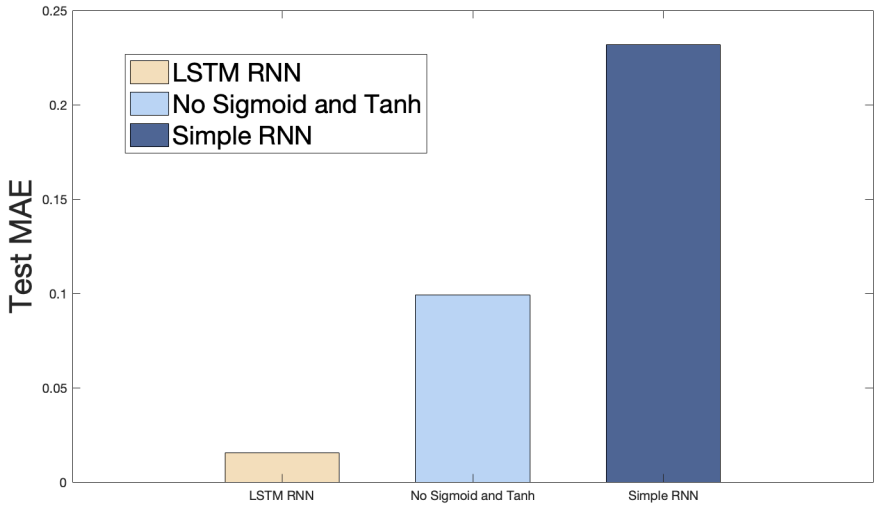

Figure 3.4: Test MAE comparison among our LSTM-RNN network, Conventional RNN and one layer LSTM-RNN

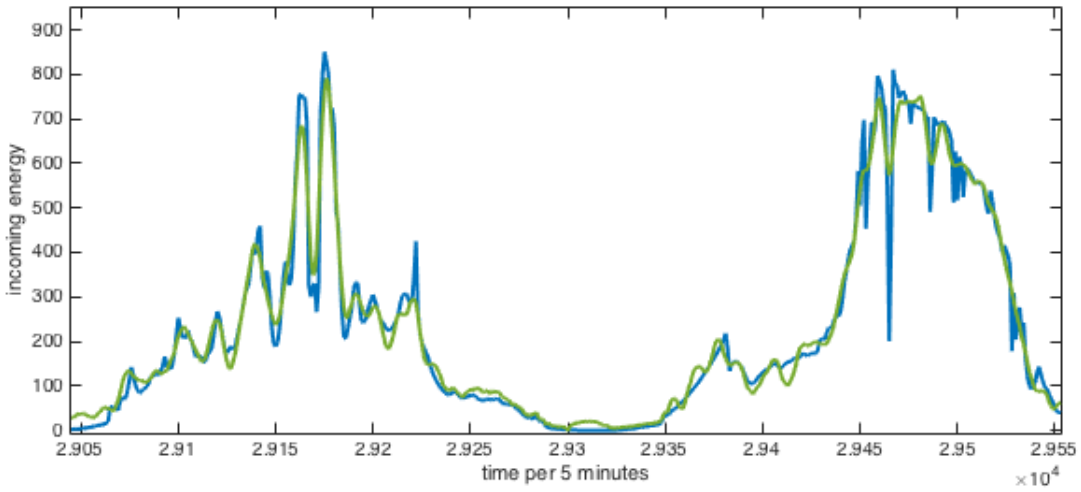

Figure 3.5: Prediction of incoming solar power generated by LSTM-RNN. Blue line: real solar energy data, Green line: solar energy prediction result

we compare the total available energy of the battery-based system and the solar powered system over the two hours experiment. In a battery-based system, we apply a common lithium battery with a size of 5.94 Wh for the sensors to work under the same monitoring task scheduling algorithm as the solar powered system. As shown in Figure 3.6, the available energy in energy harvesting mode is close to and not exceeding that in the battery-based design, which means the panel size selected is proper.

Secondly, we show the coverage comparison between battery-based heuristic algorithm, solar energy harvesting-based heuristic algorithm results and optimal assignments. As in Figure 3.7, this coverage is defined as:

$$EP\ coverage = \frac{Number\ of\ Detected\ Patterns}{Total\ Number\ of\ Patterns} \tag{3.7}$$

We increase the number of sensors from 10 to 100 to see the changes in coverage. The results of 10 sets of data in 2 hours are evaluated. The coverage increases significantly as the number of sensor grows. The performance of heuristic algorithm is slightly inferior to

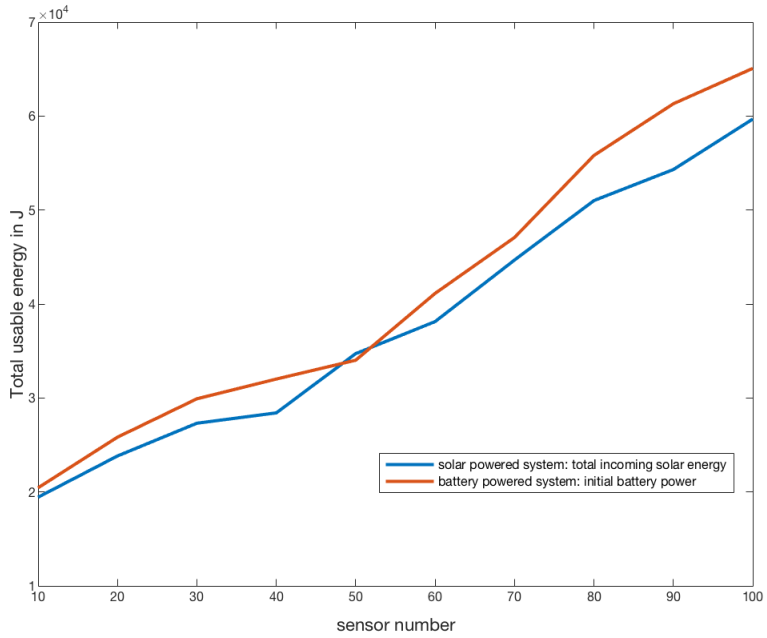

Figure 3.6: Comparison of total available energy

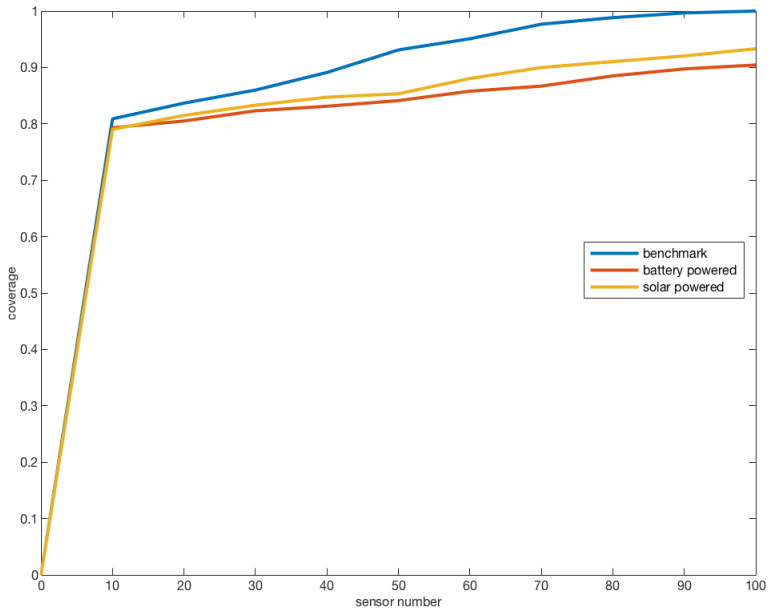

Figure 3.7: Coverage Comparison

optimal assignments due to the restricted assumptions that heuristic algorithm have, but is still within an acceptable range. We can see that the performance of solar powered system is slightly better than battery powered.

Thirdly, we show the coverage comparison at every 5 minutes in different modes as shown in Figure 3.8, The battery based system has a high coverage at first stage since initially the sensors have sufficient energy. While the performance drops sharply at a certain moment. This is because our scheduling algorithm will choose the sensor with the largest reward to perform monitoring at each assignment. Thus the performance of the system will drop drastically when the available energy to many sensors cannot support the normal operation of the system. However, in the solar powered system, we assume the sensor energy is initially zero. The sensor can only rely on the harvested energy accumulated in each step to perform monitoring, hence the performance in the early stage is relatively low. As the energy harvested by the system is increasing, the coverage at each step is gradually improved. When there is no harvestable energy in the environment, the system enters battery mode, and the performance per step is consistent with the first hour performance of battery based system.

Finally, we show the available user number changes across time. We define a sensor to be available when it has remaining energy for monitoring. A sensor is unavailable when it runs out of energy. To verify if the number of available sensors is decreasing, we define the available user ratio as:

$$Available\ User\ Ratio = \frac{Available\ User\ Number}{Total\ User\ Number} \tag{3.8}$$

and record its changes in each T_{step}. The results of 10 sets of data with different user numbers are evaluated. As shown in Figure 3.9, when the system is in energy harvesting mode (the first hour), the available user ratio of heuristic algorithm always stays 1 meaning the harvested

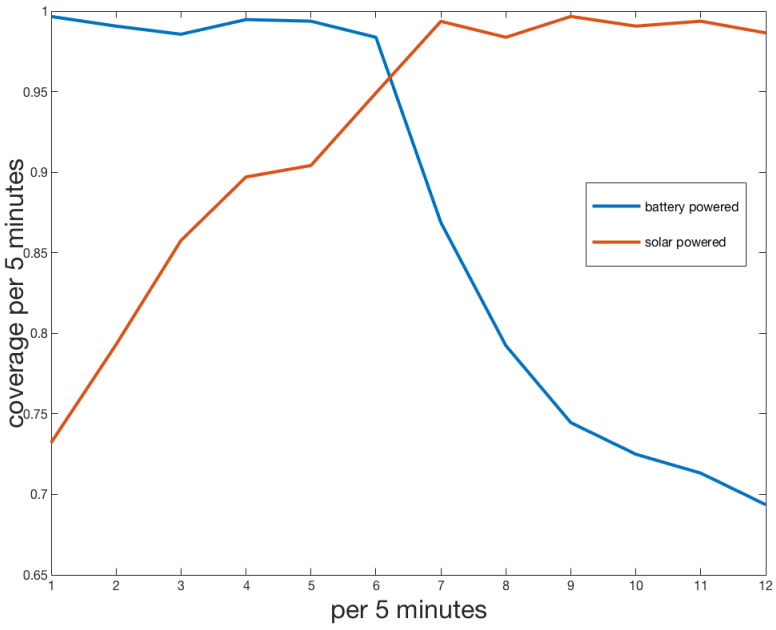

Figure 3.8: Coverage comparison at every 5 minutes

energy is adequate for sensors monitoring tasks. When the system is in battery mode (the second hour when there is no any harvestable solar energy), the number of sensors decreases, but is still in the acceptable range. Note that we only use the energy harvested within the first hour before the sunset to support the second nighttime hour's system operation. Solar energy harvested during the time right before sunset is not abundant, yet it is enough to support the system to operate normally in the battery mode which indicates that our power management scheme is reasonable.

3.6 Conclusion

In this chapter, we present a novel solar power based spectrum monitoring system consisting of multiple low cost energy-harvesting sensors. Compared with our battery-based spectrum monitoring system, we design a heuristic algorithm based on solar energy harvesting which

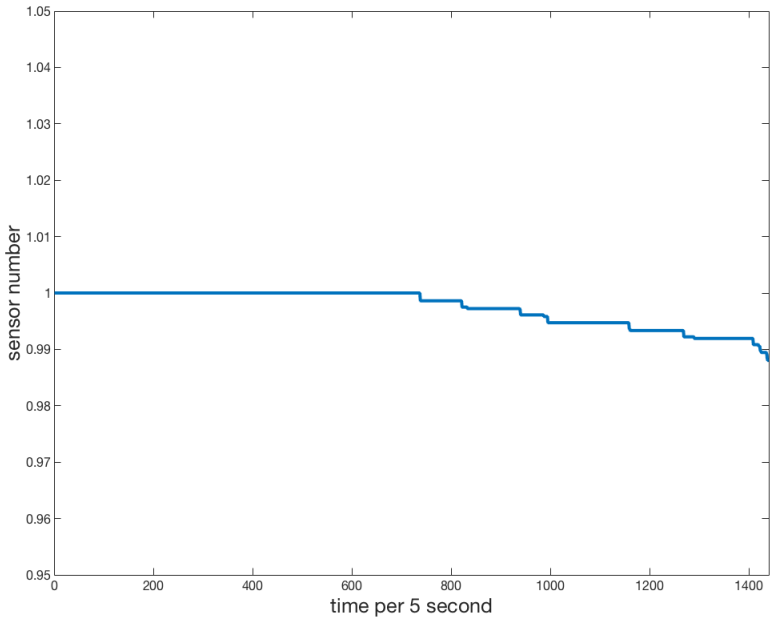

Figure 3.9: Available sensor number changes across 2 hours

can intelligently schedule the monitoring tasks by leveraging the spectrum occupancy patterns. We proposed a solar energy prediction Long short-term memory recurrent neural network to accurately predict future incoming solar power. A power management scheme is also designed for proper utilization of harvested solar power to prolong the system lifetime. We simulate the coordination among energy harvesting sensors on spectrum monitoring at large geographical scale. The simulation results show that our algorithm demonstrates a new possibility for spectrum monitoring, which could be more efficient, cheaper and more ubiquitous. The LSTM-RNN simulation results indicate our network outperforms the conventional RNN and other networks without deep layers. The power management scheme guarantees our system's functionality regardless of the absence of solar power during night time.

Chapter 4

IU's Location Privacy Protection against ESC

4.1 Introduction

4.1.1 Problem Statement

As we introduced in Section 1.2, It is currently proposed to use Environmental Sensing Capability (ESC) systems to mitigate the challenge of OPSEC. ESC is a distributed network of sensing devices used for the protection of IUs from CBSDs' transmissions [52]. ESC systems measure the received signal strength (RSS) of IU signal and provide such information to SAS. Then SAS allocates the unused frequency bands to CBSDs to avoid interference with IUs [53]. Such an ESC-based system can provide some simple and basic OPSEC protection since the location information of IUs are not revealed to SAS directly.

However, we argue that such OPSEC protection in ESC-based system is not enough for

highly sensitive IU operation data. This is because the ESC-based system still sends IU sensing results, essentially received signal strength (RSS), to SAS. The sensing results can be used to derived IUs' locations through RSS-based radio localization. This may create potential OPSEC violation if either SAS or ESCs are compromised by opponents.

4.1.2 Motivation and Contribution

In order to solve the OPSEC problem above and hide IU's true location under the detection of ESCs, in this thesis, we address it in 3.5GHz ESC-based DSA system using smart antenna on IU's side. Our design based on the fact that each ESC sensors' location and configuration are registered at FCC, which posts them for public access. Leveraging such public information, we dynamically tune the antenna gains of an IU transmitter so that even if the adversary uses an RSS-based localization scheme to derive the position of the IU, it will create uncertainty in the position of the it. Under the assumption that the adversary has full access to all ESCs sensing result, our design presents a theoretical analysis on how IU can maximize its position uncertainty. Our scheme can protect location privacy of both static and mobile IUs and it ensure the functionality of preserving whether SAS and ESCs are compromised or not.

In this work, Our group firstly formulated the problem for static IU. Due to the intractable nature of this problem, I was responsible for designing the heuristic approach based on sampling in this research work. Then we also formulate for moving IUs, in which two cases are analyzed: (1) protect IU's moving traces; (2)protect its real-time location information. Based on these formulations, I do the simulations for both static and mobile IU to analyze the feasibility of this privacy preserving problem under different circumstance by changing the number of antenna. Simulation results confirms that by adjusting IU's transmit power and antenna parameters, probability of IU's location being detected by ESCs can be reduced to a very low level. We also analyze how different IU antenna numbers, noise thresholds,

and ESCs number will influence the simulation results of IU's location privacy preserving. The results also show that our approach provides great protection for IU's location privacy. It can be proved that our analysis provides insightful advice for IU to preserve its location privacy against ESC.

4.2 Background

4.2.1 Related Work

SAS system gains received signal strength indication (RSSI) measurements of IU signals from the ESC. In an RSS-based localization system, there are significant signal receivers placed at particular locations which are used to measure the RSS of wireless nodes and report measurements to the system [54]. We refer these signal receivers as "anchors". Then the localization algorithms are used to calculate location estimates based on these measurements. In DSA, ESCs are the anchors who measure the RSS of incumbent transmitters and potentially use such information to localize the transmitter. As aforementioned, IU location privacy is highly sensitive, and therefore the question becomes: is it possible for IU to make its location or moving trajectory undiscovered even under ESCs' localization measurement?

Fortunately, most of the robust RSS-based localization schemes have limited utility no matter which statistical methods they use [55]. In many cases, there exist location spoofing methods that make wireless nodes stay undiscovered under all localization schemes. [56] shows the analysis of capability of using location spoof attacks to evade robust RSS-based localization proposals. However, [56] assumes that the radio localization system believes the targeted transmitter is leveraging omni-directional antenna and the system does not know that the transmitter can tune its antenna pattern. In addition, it does not provide any proposal

on how a radio transmitter can hide its location information. Under these circumstances, our scheme does not rely on the assumption that the adversary is unaware of to the IU's capability of radiation pattern tuning. On the contrary, our scheme provides a novel privacy preserving strategy for both static and mobile IUs.

4.2.2 System Model

Attack model

The general attack model for IU privacy in 3.5GHz is illustrated in Figure 4.1. A moving IU transmitter and multiple ESCs are distributed in a certain area. ESCs measures the RSS of IU transmission. IU can control its radiation pattern so that it can tune its antenna gains at different directions subject to the constrain of its antenna capability. The adversary has full access to all ESC sensing results and knows the IU's full capability in tuning radiation pattern. The goal of the adversary is to localize and track the IU.

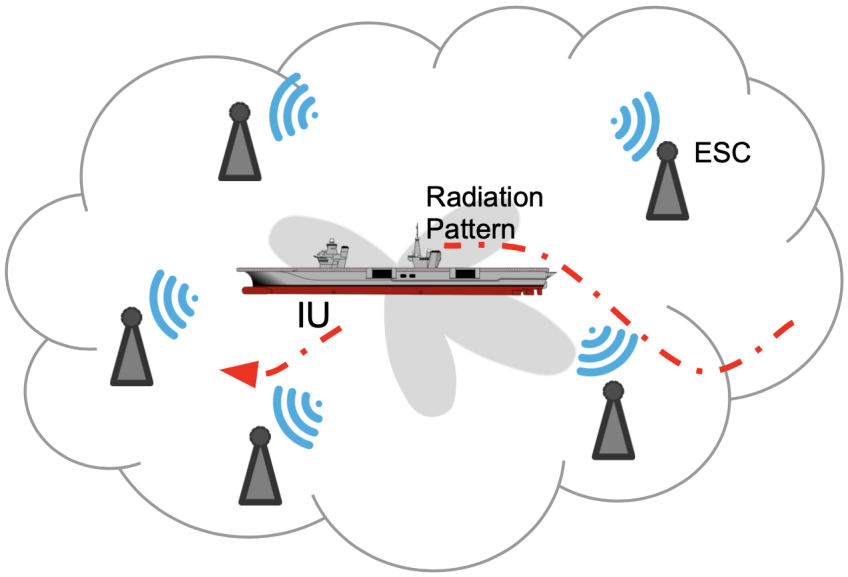

Figure 4.1: General system model

Location hiding using radiation pattern tuning

The design of our privacy preserving scheme is based on the following observation. if the node whether at location A or B can generate signals whose RSS readings are the same at the anchors, the anchors will not be able to distinguish between the two locations. Therefore, if the node at location A wants to keep itself undetected by anchors, it can make its RSS readings at anchors the same as that in location A when it is at location B. Hence, such location B becomes a fake location. When the number of fake locations increases, the true location of the node can be protected even better. Based on this, in DSA, when the area of the fake location is growing, IU can more easily hide its true location information. In this way, we are able to protect IU's location privacy.

To create such a large number of possible fake locations, IU cannot use conventional omni-directional antennas with fixed transmit power. The path loss vector from IU's location to all ESCs will be different from the path loss vectors from any other locations as long as the distance between them are different. Uniform transmit power to all directions cannot mask such location-dependent uniqueness from ESC's sensing results.

Therefore, we propose that an IU uses more advanced antenna designs, such as a smart antenna which are able to tune its radiation pattern or rotating directional antenna that can adjust its transmit power towards different directions. These advanced antenna designs are commonly found in IUs in 3.5GHz (usually military radar systems). They can vary their transmit power to different directions to mask the true path loss characteristics of its location, and then create ambiguity in ESS sensing results. Essentially, an IU in location x with radiation pattern A can create the same ESC sensing results as an IU in a large set of other possible locations with various radiation patterns by tuning of antenna gains to different direction. Our IU privacy-preserving scheme seeks to find the optimal antenna

tuning strategies that maximize the set of possible locations.

Without loss of generality, we assume that the IU is equipped with a circular smart antenna array which consists of N_{ant} isotropic elements placed over a circle with radius R. The i_{th} antenna element is located with the phase angle ϕ_i. The radiation pattern of this circular smart antenna array is expressed as [57]:

$$g(\theta, \boldsymbol{\omega}) = \sum_{i=1}^{N_{ant}} \omega_i \exp[j\frac{2\pi}{\lambda} R\cos(\theta - \phi_i)] \tag{4.1}$$

where θ represents the direction, λ is the signal wavelength and $\boldsymbol{\omega} = [\omega_1, \omega_2, ..., \omega_{N_{ant}}]^H$ is the complex weight vector which can be tuned to change the radiation pattern, and generally these weight vectors have limited range due to hardware and functionality restrictions, Thus $\omega_{min} \leq \boldsymbol{\omega} \leq \omega_{max}$.

For simplicity, let

$$\boldsymbol{h_k} = \begin{bmatrix} exp[j\frac{2\pi}{\lambda}Rcos(\theta_k - \phi_1)] \\ exp[j\frac{2\pi}{\lambda}Rcos(\theta_k - \phi_2)] \\ \vdots \\ exp[j\frac{2\pi}{\lambda}Rcos(\theta_k - \phi_{N_{ant}})] \end{bmatrix} \tag{4.2}$$

Circular antenna array is used as an example for problem illustration because it can produce flexible asymmetric radiation patterns and easily deflect a beam through 2π [56]. However, our analysis is not limited to any specific antenna model. We can plug different antenna models into the analysis by replacing Equation 4.1 with their corresponding radiation functions.

4.3 Preserving Location Privacy for Static IU

The Figure 4.2 shows the model of static IU's location preserving scheme. Respectively, the triangle refers to an IU at its true location and the square represents a possible IU location where the IU can create the same ESC sensing result as at true location. The shaded area is the union of all possible IU locations given the ESC sensing result. PL_k denotes the path loss between an IU's true location and the k_{th} ESC, and $\widehat{PL_k}$ denotes the path loss between the possible IU location and the k_{th} ESC. Pt denotes the IU's transmit power at its true location. $\widehat{Pt}$ represents the transmit power that the IU should use at the possible location. Gt_k and $\widehat{Gt_k}$ denote the antenna gain of the IU at true location and the possible location in the direction of k_{th} ESC. To simplify the procedure of contouring the possible location area, the space is segmented into grids. Each grid is represented by its center position.

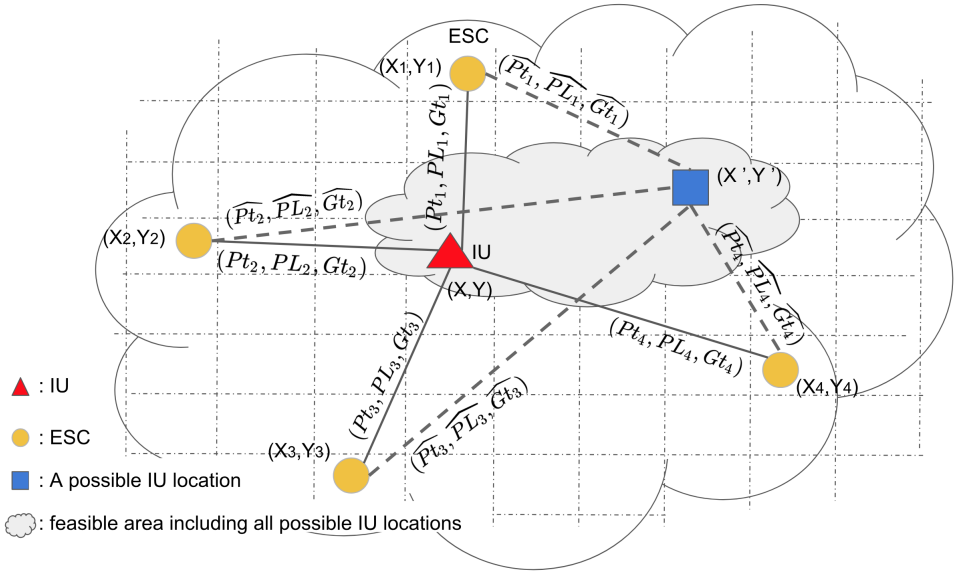

Figure 4.2: Model for static IU privacy preservation

Our analysis of tuning IU's transmitter to force the adversary to generate the largest possible IU area given ESCs' outputs are divided into two parts: (1) Compute the area of possible IU location from adversary's perspective; (2) Control the size of the area of possible IU location

by tuning the transmit power and radiation pattern or rotating directional antenna gain from IU's perspective.

From adversary's perspective

We suppose that the space is divided into N grids. There are K ESCs and their locations are represented by (x_k, y_k), $k = 1, 2, ..., K$. The true location of IU is (x, y). Each ESC will have a RSS reading from the targeted IU. The received power at k_{th} ESC from the IU at true location (x, y) is Pr_k, and the received power at k_{th} ESC if the IU is at i_{th} grid l_i is denoted by $\widehat{Pr_{i,k}}$. $\widehat{\boldsymbol{\omega}}$, $\widehat{Pt}$ represents the feasible antenna weight vector and transmit power that produce the $\widehat{Pr_{i,k}}$ approximately the same as Pr_k if IU locates at grid l_i.

After obtaining $Pr_{i,k}$ from ESCs, adversaries will determine how many grids are possible IU locations. To do this, the adversaries traverse every l_i to check if there exist a $\widehat{\boldsymbol{\omega}}$ and $\widehat{Pt}$ that make the $\widehat{Pr_{i,k}}$ approximate to Pr_k within a small noise threshold δ, suppose the IU is at that l_i. If the solution exists, this grid l_i will be determined as a possible IU location and the number of possible locations $N_{possibleLocation}$ will be added one and counted at the end. This procedure is shown in Table 4.1, where Z is the set of of the possible locations of the IU.

Table 4.1: From an adversary's perspective

given $Pr_k, \forall k = 1, 2, \cdots, K$
for each l_i, $\forall i = 1, 2, \cdots N$
  find $\widehat{\boldsymbol{\omega}}$, $\widehat{Pt}$ that satisfy: $\left| Pr_k - \widehat{Pr_{i,k}}(\widehat{\boldsymbol{\omega}}, \widehat{Pt}) \right| \leq \delta$,
  $\forall k = 1, 2, \cdots, K; i = 1, 2, \cdots N$
  if solution exists
    $N_{possibleLocation} = N_{possibleLocation} + 1$
    $Z = Z \cup l_i$

$\widehat{Pr_{i,k}}(\widehat{\boldsymbol{\omega}}, \widehat{Pt})$ is computed by:

$$\widehat{Pr_{i,k}}(\widehat{\boldsymbol{\omega}}, \widehat{Pt}) = \widehat{Pt} + \widehat{Gt_{i,k}}(\widehat{\boldsymbol{\omega}}) + PL_{i,k} + Gr - Lr \tag{4.3}$$

where $\widehat{Pt_i}$ is what the transmit power of the IU should be if it is located at l_i. Essentially, there always exists a proper range $[Pt_{min}, Pt_{max}]$ for the $\widehat{Pt_i}$ due to technical reasons, and Pt_{min} and Pt_{max} denote the minimum and maximum limits of the IU transmit power. Gr and Lr are the gain and loss at the receiver side, respectively.

$\widehat{Gt_{i,k}}(\widehat{\boldsymbol{\omega}})$ represents the feasible antenna gain of the IU if located at l_i in the direction of k_{th} ESC and computed by:

$$\widehat{Gt_{i,k}}(\widehat{\boldsymbol{\omega}}) = 10log_{10} \left| g(\theta_{i,k}, \widehat{\boldsymbol{\omega}}) \right|^2 \tag{4.4}$$

where $g(\theta, \boldsymbol{\omega})$ is the function of the antenna's radiation pattern.

In Equation 4.3, The expected path loss $PL_{i,k}$ from the center of l_i to k_{th} ESC is expressed as:

$$PL_{i,k} = 20log_{10}(\frac{4\pi}{\lambda}) + 10nlog_{10}(d_{i,k}) \tag{4.5}$$

where n represents the path loss exponent, we set $n = 2$. $d_{i,k}$ denotes the distance between l_i and k_{th} ESC, and λ denotes the transmitted wave length.

However, our analysis is not limited to this particular path loss model. It is straightforward to plug path loss models with other geometric forms into the analysis by replacing Equation 4.5 with their corresponding functions. After traversing all the grids through the procedure discussed above, adversaries are able to depict the area of possible locations for targeted IU.

From IU's perspective

In our scheme, IU tunes its transmit power Pt and antenna weight vectors $\boldsymbol{\omega}$ to control the RSS readings at ESCs to protect its location privacy. In addition, IU attempts to find a group of readings that ensures the adversaries to produce the largest area of its possible locations during localization. Here, we assume that the IU knows the locations of all surrounding ESC sensors, which are published by FCC according to 3.5 GHz regulation. This procedure of above problem is illustrated in Table 4.2. For each l_i, if there exist two groups of IU parameters, $\boldsymbol{\omega}$ and Pt for IU at true location and $\widehat{\boldsymbol{\omega}}$ and $\widehat{Pt}$ for IU at l_i, that makes the corresponding $Pr_k(\boldsymbol{\omega}, Pt)$ and $\widehat{Pr_{i,k}}(\widehat{\boldsymbol{\omega}}, \widehat{Pt})$ at ESCs approximately the same, the IU confirms this l_i to be a possible IU location and increases the count of possible locations $N(\boldsymbol{\omega}, Pt)_{possibleLocation}$. Finally, the IU can obtain a set of $\boldsymbol{\omega}$s and Pts that maximize the $N(\boldsymbol{\omega}, Pt)_{possibleLocation}$, and these $\boldsymbol{\omega}$s and Pts are the optimal choices for IU's transmit power and antenna weight vector.

Table 4.2: From IU's perspective

for each l_i, $\forall i = 1, 2, \cdots N$
find $\boldsymbol{\omega}$, Pt, $\widehat{\boldsymbol{\omega}}$, $\widehat{Pt}$:
$\boldsymbol{\omega}, \widehat{\boldsymbol{\omega}} \in [\omega_{min}, \omega_{max}]$, $Pt, \widehat{Pt} \in [Pt_{min}, Pt_{max}]$
that satisfy: $\left\|Pr_k(\boldsymbol{\omega}, Pt) - \widehat{Pr_{i,k}}(\widehat{\boldsymbol{\omega}}, \widehat{Pt})\right\| \leq \delta$,
$\forall k = 1, 2, \cdots, K; i = 1, 2, \cdots N$
if solution exists
$N(\boldsymbol{\omega}, Pt)_{possibleLocation} =$
$N(\boldsymbol{\omega}, Pt)_{possibleLocation} + 1$
$Z(\boldsymbol{\omega}, Pt) = Z(\boldsymbol{\omega}, Pt) \cup l_i$
$\boldsymbol{\omega}_{opt}, Pt_{opt} = \arg\max_{\boldsymbol{\omega}, Pt} N(\boldsymbol{\omega}, Pt)_{possibleLocation}$

4.4 Solving the problem: Heuristic Algorithm

Since the problem of preserving static IU's location privacy's formulation need to search over continuous variable spaces, which is generally NP-hard (The proof of NP-hard problem is shown in paper "Preserving Incumbent Use's Location Privacy Against Environmental Sensing Capabilities" that we are working on), we cannot obtain the optimal solution by directly solving it. Therefore, in this section, we introduce a heuristic algorithm whose results approximate the optimal solutions. We then explain the worst case which our algorithm cannot handle and provide an analysis on how to determine whether the worst case will happen at given circumstances.

To decide if a grid l_i is a possible IU location, we uniformly sample each variable into discrete points such that $\boldsymbol{\omega} \in [\boldsymbol{\omega}_1, \boldsymbol{\omega}_2, \cdots, \boldsymbol{\omega}_{N_1}]$, $\widehat{\boldsymbol{\omega}} \in [\widehat{\boldsymbol{\omega}}_1, \widehat{\boldsymbol{\omega}}_2, \cdots, \widehat{\boldsymbol{\omega}}_{N_1}]$, $Pt \in [Pt_1, Pt_2, \cdots, Pt_{M_1}]$, $\widehat{Pt} \in [\widehat{Pt}_1, \widehat{Pt}_2, \cdots, \widehat{Pt}_{M_1}]$. We define a tuple $U_i = [\boldsymbol{\omega}_{n_1}, Pt_{n_2}, \widehat{\boldsymbol{\omega}}_{m_1}, \widehat{Pt_{m_2}}]$ ($\forall n_1, m_1 \in [1, N_1]$, $n_2, m_2 \in [1, M_1]$, $i \in [1, N_1^2 N_2^2]$) as a group of sampled variables. This is reasonable because precision of the hardware is always finite. Then a brute-force algorithm is adopted to search for the optimal points which maximize the number of possible IU locations. This procedure is illustrated in Table 4.3.

If the variable space is sampled finely enough, we can approach the optimal solution boundlessly. Apparently, the accuracy of the heuristic algorithm is closely related to the sampling interval. In our algorithm, we first sample the variable spaces and traverse all the tuples of sampled variables for each l_i and each ESC to determine whether it is a possible location for IU. Hence we want to measure the impact of sampling in our algorithm. The worst case occurs when all discrete points cannot satisfy the condition in Table 4.2, while feasible points do exist within the scale interval. Only this case leads to the sampling error in our algorithm. To analyze this error, we attempt to answer two questions: Can we determine

Table 4.3: Heuristic Algorithm

suppose IU is at location (x, y)
for each l_i, $\forall i = 1, 2, \cdots N$
  for each tuple $U_i = [\boldsymbol{\omega}_{n_1},\ Pt_{n_2},\ \widehat{\boldsymbol{\omega}}_{m_1},\ \widehat{Pt}_{m_2}\ ]$
  $\forall n_1, m_1 \in [1, 2, \cdots, N_1]$, $n_2, m_2 \in [1, 2, \cdots, M_1]$
    compute $\text{diff}_k = \left| Pr_k(\boldsymbol{\omega}_{n_1}, Pt_{n_2}) - \widehat{Pr_{i,k}}(\widehat{\boldsymbol{\omega}}_{m_1}, \widehat{Pt}_{m_2}) \right|$
    $\forall k = 1, 2, \cdots, K$
    if $|\text{diff}_k| \leq \delta$, $\forall k = 1, 2, \cdots, K$
    /* count the number of possible locations
    corresponding to each IU configuration */
    $N(\boldsymbol{\omega}_{n_1}, Pt_{n_2})_{possibleLocation} =$
      $N(\boldsymbol{\omega}_{n_1}, Pt_{n_2})_{possibleLocation} + 1$
    /* record the area of possible locations
    corresponding to each IU configuration */
    $Z(\boldsymbol{\omega}_{n_1}, Pt_{n_2}) = Z(\boldsymbol{\omega}_{n_1}, Pt_{n_2}) \cup l_i$
  ($Z(\boldsymbol{\omega}_n, Pt_n)$: possible IU area given $\boldsymbol{\omega}_n, Pt_n$)

$\boldsymbol{\omega}_{opt}, Pt_{opt} = \arg\max_{\boldsymbol{\omega}, Pt} N(\boldsymbol{\omega}, Pt)_{possibleLocation}$

when the worst case will happen? And how?

Let us look at a simple scenario for the worst case. Suppose for k_{th} ESC and l_i, we cannot find any $\boldsymbol{\omega}, Pt, \widehat{\boldsymbol{\omega}}, \widehat{Pt}$ that makes l_i a possible IU location. That is, any tuple $U_i = [\boldsymbol{\omega}_{n_1}, Pt_{n_2}, \widehat{\boldsymbol{\omega}}_{m_1}, \widehat{Pt_{m_2}}]$ will not meet the condition in Table 4.2. However, feasible point exists between tuples at $[\boldsymbol{\omega}_{n_1}+\Delta\boldsymbol{\omega},\ Pt_{n_2}+\Delta p,\ \widehat{\boldsymbol{\omega}}_{m_1}+\widehat{\Delta\boldsymbol{\omega}},\ \widehat{Pt_{m_2}}+\widehat{\Delta p}]$, where $\Delta\boldsymbol{\omega}, \Delta p, \widehat{\Delta\boldsymbol{\omega}}, \widehat{\Delta p}$ are small portions of the corresponding scale intervals $\Delta p_{max} = p_0$, $\Delta\widehat{\omega_{max}} = \widehat{\omega_0}$, $\Delta p_{max} = p_0$, $\Delta\widehat{\omega_{max}} = \widehat{\omega_0}$. Note that when $\Delta\boldsymbol{\omega}, \Delta p, \widehat{\Delta\boldsymbol{\omega}}, \widehat{\Delta p}$ equal to 0 or the entire scale intervals, the point at $[\boldsymbol{\omega}_{n_1} + \Delta\boldsymbol{\omega},\ Pt_{n_2} + \Delta p,\ \widehat{\boldsymbol{\omega}}_{m_1} + \widehat{\Delta\boldsymbol{\omega}}, \widehat{Pt_{m_2}} + \widehat{\Delta p}]$ then becomes a tuple of sampled variables. For example, tuple $[\boldsymbol{\omega}_{n_1} + \Delta\boldsymbol{\omega}_{max},\ Pt_{n_2} + \Delta p_{max},\ \widehat{\boldsymbol{\omega}}_{m_1} + \widehat{\Delta\boldsymbol{\omega}_{max}}, \widehat{Pt_{m_2}} + \widehat{\Delta p_{max}}]$ equals to tuple $[\boldsymbol{\omega}_{n_1+1},\ Pt_{n_2+1},\ \widehat{\boldsymbol{\omega}}_{m_1+1}, \widehat{Pt_{m_2+1}}]$.

Given above assumptions, we have a group of inequalities as follow:

$$\begin{cases} \left| Pr_k(\boldsymbol{\omega}_{n_1}, Pt_{n_2}) - \widehat{Pr_{i,k}}(\widehat{\boldsymbol{\omega}_{\boldsymbol{m_1}}}, \widehat{Pt_{m_2}}) \right| > \delta, \\ \forall n_1, m_1 \in [1, N_1],\ \forall n_2, m_2 \in [1, M_1] \\ |Pr_k(\boldsymbol{\omega}_{n_1} + \Delta\boldsymbol{\omega}, Pt_{n_2} + \Delta p) - \widehat{Pr_{i,k}}(\widehat{\boldsymbol{\omega}}_{m_1} + \widehat{\Delta\boldsymbol{\omega}}, \widehat{Pt_{m_2}} \\ +\widehat{\Delta p})| \leq \delta, \exists n_1, m_1 \in [1, N_1],\ n_2, m_2 \in [1, M_1] \\ 0 \leq \Delta p \leq p_0 \\ 0 \leq \Delta\boldsymbol{\omega} \leq \omega_0 \\ 0 \leq \widehat{\Delta p} \leq \widehat{p_0} \\ 0 \leq \widehat{\Delta\boldsymbol{\omega}} \leq \widehat{\omega_0} \end{cases} \tag{4.6}$$

Since we assume at least a feasible point exists between tuple $U_i = [\boldsymbol{\omega}_{n_1}, Pt_{n_2}, \widehat{\boldsymbol{\omega}}_{m_1}, \widehat{Pt_{m_2}}]$ and its surrounding tuples at $[\boldsymbol{\omega}_{n_1} + \Delta\boldsymbol{\omega},\ Pt_{n_2} + \Delta p,\ \widehat{\boldsymbol{\omega}}_{m_1} + \widehat{\Delta\boldsymbol{\omega}}, \widehat{Pt_{m_2}} + \widehat{\Delta p}]$, to find the $\Delta\boldsymbol{\omega}, \Delta p, \widehat{\Delta\boldsymbol{\omega}}, \widehat{\Delta p}$ that can solve these inequalities, we define a function f_{U_i} for tuple U_i as:

$$\begin{aligned} & f_{U_i}(\Delta\boldsymbol{\omega}, \Delta p, \widehat{\Delta\boldsymbol{\omega}}, \widehat{\Delta p}) := \\ & Pr_k(\boldsymbol{\omega}_{n_1} + \Delta\boldsymbol{\omega}, Pt_{n_2} + \Delta p) - \widehat{Pr_{i,k}}(\widehat{\boldsymbol{\omega}_{m_1}} + \widehat{\Delta\boldsymbol{\omega}}, \widehat{Pt_{m_2}} + \widehat{\Delta p}) \\ & = \ln \left[(Pt_{n_2} + \Delta p) \left(\sum_{I=1}^{N_{ant}} (\omega_{n_1,I} + \Delta\omega_I) C_I \right)^2 \right] \\ & \quad - \ln \left[(\widehat{Pt_{m_2}} + \widehat{\Delta p}) \left(\sum_{I=1}^{N_{ant}} (\widehat{\omega_{m_1,I}} + \widehat{\Delta\omega_I}) \widehat{C_I} \right)^2 \right] \end{aligned} \tag{4.7}$$

where $C_I = \sqrt{PL_{i,k}} \exp[j\frac{2\pi}{\lambda} R\cos(\theta - \phi_I)]$ if using circular phased array antenna.

If there exists at least a $f_{U_i}(\Delta\boldsymbol{\omega}, \Delta p, \widehat{\Delta\boldsymbol{\omega}}, \widehat{\Delta p}) = f_0$ that satisfies $-\delta \leq f_0 \leq \delta$, the inequalities are solvable, and the worst case happens.

To analyze the characteristics of $f_{U_i}(\Delta\boldsymbol{\omega}, \Delta p, \widehat{\Delta\boldsymbol{\omega}}, \widehat{\Delta p})$, we first compute the partial derivative for each variable Δp, $\widehat{\Delta p}$, $\Delta\omega_j$ and $\widehat{\Delta\omega_j}$ ($j \in [1, N_{ant}]$):

$$
\begin{aligned}
\frac{\partial f}{\partial \Delta p} &= \frac{1}{Pt_{n_2} + \Delta p} > 0 \\
\frac{\partial f}{\partial \widehat{\Delta p}} &= -\frac{1}{\widehat{Pt_{m_2}} + \widehat{\Delta p}} < 0 \\
\frac{\partial f}{\partial \Delta \omega_j} &= \frac{2C_j}{\sum_I^{N_{ant}} (\omega_{n_1,I} + \Delta\omega_I) C_I} > 0 \\
\frac{\partial f}{\partial \widehat{\Delta \omega_j}} &= -\frac{2\widehat{C_j}}{\sum_I^{N_{ant}} (\widehat{\omega_{m_1,I}} + \widehat{\Delta\omega_I})\widehat{C_I}} < 0
\end{aligned}
\tag{4.8}
$$

As we can see, $f_{U_i}(\Delta\boldsymbol{\omega}, \Delta p, \widehat{\Delta\boldsymbol{\omega}}, \widehat{\Delta p})$ is monotonically increasing at $\Delta\boldsymbol{\omega}$ and Δp and monotonically decreasing at $\widehat{\Delta\boldsymbol{\omega}}, \widehat{\Delta p}$. Therefore, the maximum of $f_{U_i}(\Delta\boldsymbol{\omega}, \Delta p, \widehat{\Delta\boldsymbol{\omega}}, \widehat{\Delta p})$ is determined as

$$f_{max} = f_{U_i}(\Delta\boldsymbol{\omega}_{max}, \Delta p_{max}, \widehat{\Delta\boldsymbol{\omega}}_{min}, \widehat{\Delta p}_{min}) = f_{U_{j1}}(0,0,0,0),$$

where tuple $U_{j1} =$

$$[\boldsymbol{\omega}_{n_1} + \Delta\boldsymbol{\omega}_{max}, Pt_{n_2} + \Delta p_{max}, \widehat{\boldsymbol{\omega}}_{m_1} + \widehat{\Delta\boldsymbol{\omega}}_{min}, \widehat{Pt_{m_2}} + \widehat{\Delta p}_{min}]$$

$$= [\boldsymbol{\omega}_{n_1+1}, Pt_{n_2+1}, \widehat{\boldsymbol{\omega}_{m_1}}, \widehat{Pt_{m_2}}],$$

and the minimum can be found at

$$f_{min} = f_{U_i}(\Delta\boldsymbol{\omega}_{min}, \Delta p_{min}, \widehat{\Delta\boldsymbol{\omega}}_{max}, \widehat{\Delta p}_{max}) = f_{U_{j2}}(0,0,0,0).$$

where tuple $U_{j2} =$

$$[\boldsymbol{\omega}_{n_1} + \Delta\boldsymbol{\omega}_{min}, Pt_{n_2} + \Delta p_{min}, \widehat{\boldsymbol{\omega}}_{m_1} + \widehat{\Delta\boldsymbol{\omega}}_{max}, \widehat{Pt_{m_2}} + \widehat{\Delta p}_{max}]$$

$$= [\boldsymbol{\omega}_{n_1}, Pt_{n_2}, \widehat{\boldsymbol{\omega}_{m_1+1}}, \widehat{Pt_{m_2+1}}],$$

Therefore, f_{max} is obtained at tuple U_{j1},

$$f_{max} = Pr_k(\boldsymbol{\omega}_{n_1+1}, Pt_{n_2+1}) - \widehat{Pr_{i,k}}(\widehat{\boldsymbol{\omega}_{m_1}}, \widehat{Pt_{m_2}}),$$

and f_{min} is obtained at tuple U_{j2},

$$f_{min} = Pr_k(\boldsymbol{\omega}_{n_1}, Pt_{n_2}) - \widehat{Pr_{i,k}}(\widehat{\boldsymbol{\omega}_{m_1+1}}, \widehat{Pt_{m_2+1}}).$$

According to the assumptions, there are three cases for f_{max} and f_{min}:

1. $f_{min} \leq f_{max} < -\delta$: since we cannot find any f_0 between f_{max} and f_{min} that satisfies $-\delta \leq f_0 \leq \delta$, and thus the inequalities are infeasible.

2. $f_{max} \geq f_{min} > \delta$: same as above.

3. $f_{max} > \delta$ and $f_{min} < -\delta$: since f_{max} and f_{min} are obtained at tuples U_{j1} and U_{j2} respectively, according to the assumption that every tuple U_i will lead to $|f_{U_i}| > \delta$, there must be a set of solutions that satisfies $-\delta \leq f_0 \leq \delta$, and thus only in this case the inequalities are feasible such that the worst case happens.

Therefore, for k_{th} ESC, if all tuples of sampled variables cannot make l_i a possible IU location, whether a worst case exists between $\boldsymbol{\omega}_{n_1}, Pt_{n_2}$ and $\widehat{\boldsymbol{\omega}_{m_1}}, \widehat{Pt_{m_2}}$ ($\forall n_1, m_1 \in [1, N_1]$, $\forall n_2, m_2 \in [1, M_1]$) can be examined directly using the value of

$$Pr_k(\boldsymbol{\omega}_{n_1}, Pt_{n_2}) - \widehat{Pr_{i,k}}(\widehat{\boldsymbol{\omega}_{m_1+1}}, \widehat{Pt_{m_2+1}})$$

and

$$Pr_k(\boldsymbol{\omega}_{n_1+1}, Pt_{n_2+1}) - \widehat{Pr_{i,k}}(\widehat{\boldsymbol{\omega}_{m_1}}, \widehat{Pt_{m_2}}),$$

if the values satisfy the condition in third case, we can say that the worst case exists between $\boldsymbol{\omega_{n_1}}$,$Pt_{n_2}$ and $\widehat{\boldsymbol{\omega}_{m_1}}, \widehat{Pt_{m_2}}$, or otherwise it does not.

4.5 Preserving Location Privacy for Moving IUs

We have discussed how to protect the static IU location. However, it is also critical to protect moving IU location privacy since IUs like shipborne radar are often mobile. Same as in the

static IU model, adversaries have the capability to calculate the area where IU may appear at each moment using both current and historical RSS readings at ESCs. Meanwhile, they can also estimate the IU's possible moving ranges based on the feasible range of IU speed.

our scheme tunes an IU's transmit power and radiation pattern during movement to optimally preserve its privacy, assuming that the IU knows its future moving route. The design of our scheme is based on the relation between IU's tunable parameters and the adversary's estimation of the possible moving traces of IU. We assume the IU can adjust its transmit power and radiation pattern at any moment subject to hardware restrictions on its functionality.

Model for moving IU is the same as in Figure 4.2 except that the IU is mobile in this case. Consider a discrete time range $T = [t_1, ..., t_n]$, where each time slot t_i is of the same size. During time T, IU is moving along a planned route and ESCs detect the IU's signal and record the RSS readings at each time slot. From these RSS readings, the possible IU area at a time slot $t_i \in T$ can be computed and is denoted as Z_i. Computing Z_t is different from Section 4.3's computation of the area of static IU possible locations. This is because the adversary has access to historical RSS data and there is realistic upper limit on IU moving speed. From the adversary's point of view, the past possible location area Z_{i-1} constrains the possible locations of IU at current time t_i because the distances between possible locations cannot be larger than an IU's maximum moving speed times a time slot. For example, the shape of Z_1 will restrict the area of Z_2, and the shrunken Z_2 will further impact Z_3. Conversely, feasible area of possible IU locations at current time t_i (i.e. Z_i) will also cause shrinking of the possible IU area estimation for previous time slots. This essentially means that the current Z_i will also reduce Z_{i-1} to Z_1, essentially restricting the size of the past moving trajectory. The algorithm in Table 4.4 shows how the adversary can narrow down the possible location traces of moving IUs through such correlation between historical location estimation and current location estimation. In this algorithm, the adversary assumes the

maximum speed of IU is Δ per time interval.

Table 4.4: Adversary generates possible areas for moving IU

At the current time t_n:
Given the RSS readings at t_n
Step 1: Compute initial estimation of Z_n using RSS readings according to Table 4.1 in Section 4.3.
Step 2: /* update current Z_n by Z_{n-1} */
$Z_n = \{l_i \| l_i \in Z_n$ and $\exists l_j \in Z_{n-1}$such that$\|l_i - l_j\| \leq \Delta\}$
Step 3: /* Update past location trajectory based on Z_n*/
From $t_j = t_{n-1}$ to $t_j = t_1$:
$Z_j = \{l_k \| l_k \in Z_j$ and $\exists l_u \in Z_{j+1}$such that$\|l_k - l_u\| \leq \Delta\}$

Then we must consider the correlation between past moving trajectory and current location estimation. Hence, selecting the optimal IU transmit parameters at each time slot is not equivalent to find one single global optimal parameters for the entire time period. Instead, an IU must dynamically tune its antenna patterns and transmit power at each slot to defend its moving trajectory and current location. Next, we will present our analysis about (1) how IU can hide its true moving trajectories; (2) how IU can hide its real-time current location.

(1) We know that an IU can change the RSS readings at ESC side by adjusting its transmit power and radiation pattern, so that it can control adversary's estimation on the area of possible IU locations. Thus, assuming the IU knows its future route, it can make a plan of how to adjust these tunable parameters along its way to reduce the adversary's probability on finding out the IU's true trace. We define this probability as a summation of the reciprocal of the size of possible IU area Z_t ($\forall\ t \in [t_1, t_n]$) for every time slot in T. The goal is to find the best plan of transmit power and antenna weight vector for IU at every time slot that minimize this probability, as formulated as:

$$opt\_\boldsymbol{\omega_j}, opt\_Pt_{j,j\in[1,n]} = \underset{\boldsymbol{\omega_j}, Pt_j, j\in[1,n]}{\arg\min} \sum_{j=1}^{n} \frac{1}{size(Z_j(\boldsymbol{\omega_j}, Pt_j))} \tag{4.9}$$

Here, we assume the adversary will use the algorithm in Table 4.4 to compute Z_j and the IU can estimate the RSS readings at ESCs for each of its future location.

We can compute Equation 4.9 in four steps. Step 1: Discretizes the IU's future route plan into a series of points, where a point L_i corresponds to the planed IU position at time t_i. Step 2: For each location point L_i, run algorithm in Table 4.3 to compute the set of $Z_i(\boldsymbol{\omega}_{n_1}, Pt_{n_2})$, which is the collection of possible location areas for each possible IU configuration at time t_i. Denote the set as $\widetilde{Z}_i = \{Z_i(\boldsymbol{\omega}_{n_1}, Pt_{n_2})|$ for all $(\boldsymbol{\omega}_{n_1}, Pt_{n_2})\}$. Step 3: For every possible sequence of IU parameter tuning, which is denoted as $s = \{(\omega_{n_1}, Pt_{n_2})_i | i = 1...n\}$, retrieve the corresponding sequence of Z_i and narrow down these Z_i based on Step 2 and 3 in Table 4.4. Step 4: Pick the best sequence S_{opt} that satisfies Equation 4.9 among all sequences.

(2) Consider that an adversary is using the algorithm in Table 4.4 to obtain the feasible area of possible IU locations at any moment given the IU parameters. If the IU wants to best conceal its location at a current time t_n, it needs to find a certain group of IU parameters that minimize the probability on finding out its true location at t_n, which can be formulated as minimizing the reciprocal of Z_n as follows:

$$opt\_\boldsymbol{\omega}_n, opt\_Pt_n = \arg\min_{\boldsymbol{\omega}_n, Pt_n} \frac{1}{size(Z_n(\boldsymbol{\omega}_n, Pt_n))} \tag{4.10}$$

An four steps' algorithm similar to the one in last analysis can be used to find the solution for this goal. The only change is in Step 4, where the metric of selecting the optimal tuning sequence should be Equation 4.10 instead of Equation 4.9.

4.6 Simulation

In this section, we simulate the static IU and the moving IU location privacy protection problem described in Section 4.3 and 4.5 to analyze the feasibility of our privacy-protection scheme under different circumstances. Our simulation confirms that by adjusting IU's transmit power and antenna's radiation pattern, probability of IU's location being detected by adversaries using ESCs' sensing outputs can be reduced to a very low level. We also analyze how different numbers of antenna elements, noise thresholds, and ESCs number will influence the simulation results for preserving IU's location privacy.

Simulation results for static IU using circular phased array antenna are shown in Figure 4.3. The parameters used in this simulation are $N_{ant} = 2$ or 5, $\delta = 2dB$, $K = 4$, the grid length is set to 100 m. In Figure 4.3, the circle represents a true IU location, the plus represent the ESCs' locations and asterisk represents the possible IU locations produced by adversaries. We can see that true IU location is successfully hidden inside the computed possible locations. It is not surprising that the areas close around true location will have high probabilities to be a possible IU location, and the simulation results proved this speculation. However, there are many points very far away from true location that still end up as possible IU locations, which shows the strong feasibility for preserving IU's static location privacy.

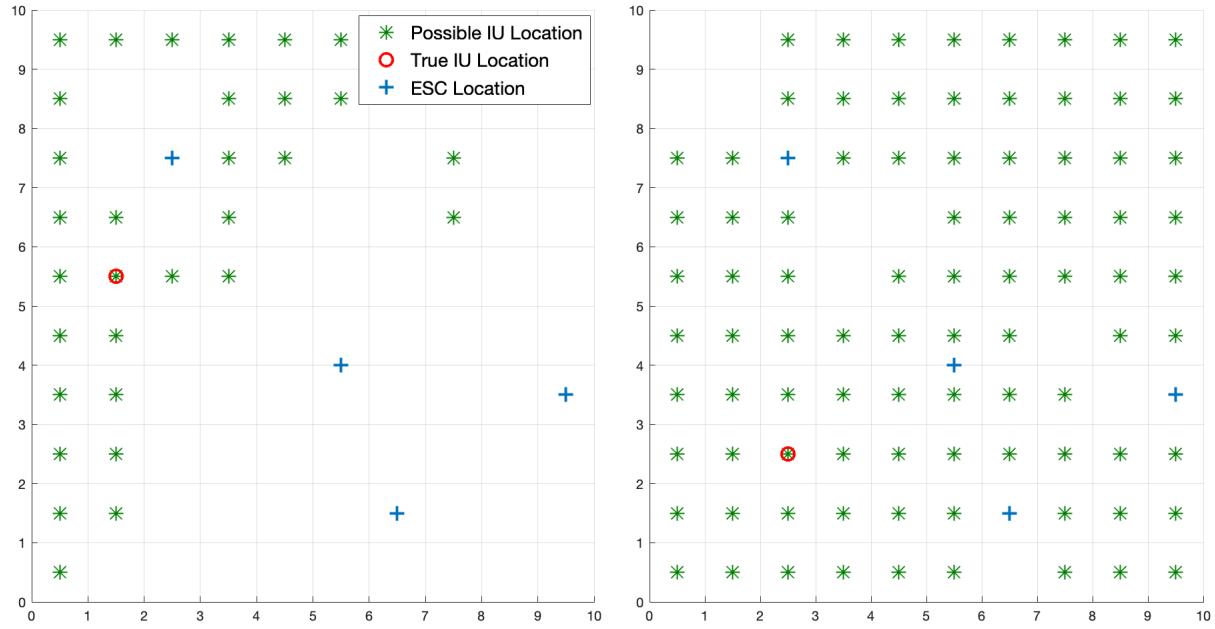

Figure 4.3: Examples showing maximized possible location area for static IU when $N_{ant} = 2$ and $N_{ant} = 5$.

In our simulation of mobile IUs, we set the speed of IU as between 0 to 2 (grid per time interval). Figure 4.4 shows an example of possible IU locations at 6 consecutive points of time while IU is moving, where N_{ant} is set to 2 and the number of K is 4. As in each sub-figure, IU is successfully hidden within a bunch of possible IU locations. Though the possible locations tend to appear around the true IU location, many of them also exist in distant grids, which is another positive factor to preserve moving IU's location privacy.

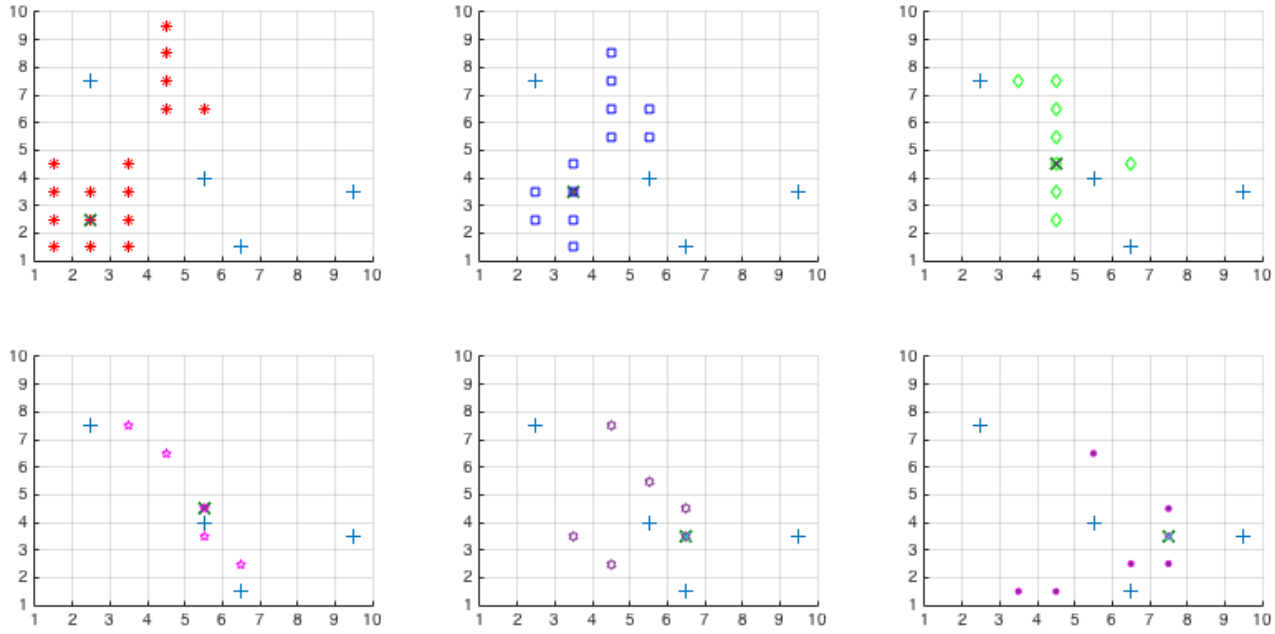

Figure 4.4: Maximal areas of possible IU locations at each point of time. The cross in all the sub-figures denotes true IU location, the plus denotes the ESC locations, and the others are computed possible IU locations.

Figure 4.5 shows 10 randomly picked possible traces for one IU's real route (There are many more that we cannot show for figure clarity reason). We can see that merely using 2 antenna elements IU can still befog ESCs with many fake traces.

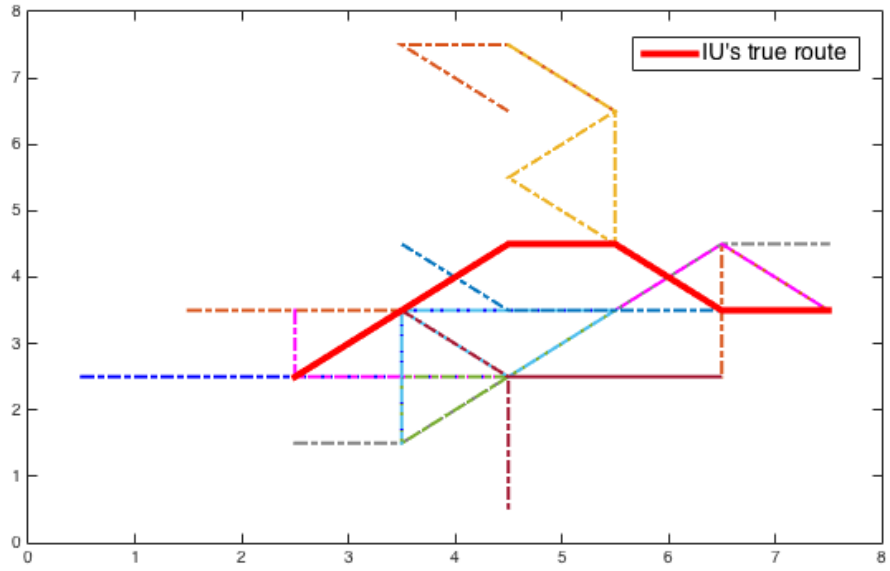

Figure 4.5: 10 randomly picked possible IU traces in dash-dot lines and the IU's real route in a sold red line.

The most dissimilar traces and the most similar traces (except the true route) to the true route of IU are presented in Figure 4.6. We measure the similarity between two traces by:

$$dist = \sum_{t=t_1}^{t_n} \sqrt{(L1_t - L2_t)^2} \tag{4.11}$$

where n is the number of time points of these two traces, and $L1_t$ denotes the location of trace 1 at time t ($t \in [t_1, t_n]$), $L2_t$ denotes the location of trace 2 at time t. As in Figure 4.6, the existence of these possible traces that are far away from the true trace as shown in Figure 4.4 makes preservation of moving IU's location privacy feasible.

Table 4.5 shows the number of possible IU trajectories computed under five different routes

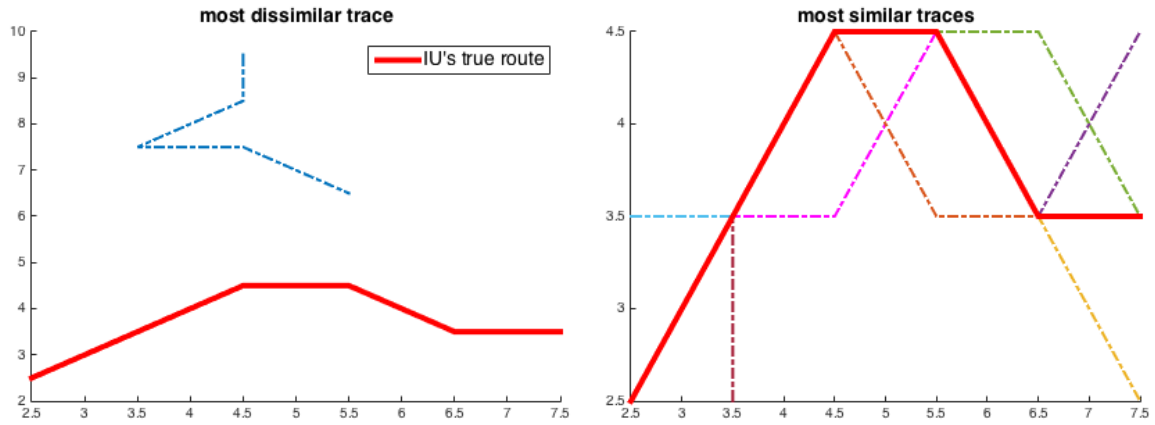

Figure 4.6: An example showing the most dissimilar trace and the most similar traces.

of the IU, and the amount of possible trajectories varies much on different IU routes. The maximal distance refers to the similarity between true IU route and possible traces. It is computed by Equation 4.11. The total distance between a true route and a possible trace within 6 points of time is as large as thousands. The average Euclidean distance (max dist./6 time points) between true IU trace and possible IU trace is usually larger than 200m.

Table 4.5: Number of possible IU trajectories computed under five different routes of the IU

IU routes number	1	2	3	4	5
possible routes	2567	2158	7169	4443	13935
max dist. (×100m)	14.36	16.99	15.63	22.39	31.88

Next, we assume IU moves within 6 time steps, and record the number of possible IU locations at last time step which can be regarded as possible current locations for IU. We also record the number of possible IU traces along the way. Three general trends in Table 4.6 and Table 4.7 can be observed. First, both the number of possible current IU locations and the number of possible IU trajectories increases when the number of antenna elements N_{ant} increases. This is because smart antenna array with more elements has more flexibility in adjusting the radiation pattern. Mathematically, more antenna elements leads to more tunable $\boldsymbol{\omega}$ and hence larger degree of freedom in the problems, so that it is easier for IU

to create different RSS readings at ESCs. Second, the number of possible IU locations and trajectories also increases as the value of acceptable noise level increases. The reason is that larger noise level indicates looser bounds in determining a possible IU location. Third, both the numbers of possible IU locations at last time step and possible IU trajectories decrease when the number of ESCs (i.e. K) grows. Mathematically, adding ESCs means adding extra constraints to problem in Table 4.2, and further reduce the l_i's probability of being regarded as a possible IU location.

Table 4.6: Number of possible IU traces

δ	K	$N_{ant} = 2$	$N_{ant} = 5$
1 dB	4	66	6861103
	6	22	5524652
2 dB	4	2567	11082980
	6	357	10037580

Table 4.7: Number of possible current locations for IU

δ	K	$N_{ant} = 2$	$N_{ant} = 5$
1 dB	4	4	72
	6	3	71
2 dB	4	10	89
	6	8	87

4.7 Conclusion

In this chapter, we analyzed the feasibility of preserving both static and moving IU's location privacy by adjusting its radiation pattern and transmit power. We defined the way to preserve IU's location privacy as to hide its true location inside all other possible IU locations estimated by adversaries using ESCs' RSS readings. We investigated how IU's transmit power, radiation pattern and ESC deployment influence IU's capability of hiding its location.

We formulated the problem for static IU to protect its location information whose feasibility is NP-hard in general, and hence we proposed a sampling method to solve this problem. Based on this, we then formulated the problem for moving IUs, in which two cases are analyzed: the first is to protect IU's moving traces and the second is to protect its real-time location information. Our analysis provides insightful guidance for IU to preserve its location information no matter when it is static or moving against the potential localization attack of ESCs. Simulation results also show that our approach provides great effectiveness for IU's location privacy protection.

Chapter 5

Conclusion

For the two major technical challenges in Dynamic Spectrum Access system, we put forward targeted improvement suggestions and schemes. In chapter 2, we proposed a crowdsourcing-based spectrum monitoring system. In order to achieve the highest spectrum monitoring coverage with the limited energy and changing number of mobile users, we leverage the IU occupancy pattern to show the spectrum access behaviours. Our system uses a smart scheduling algorithm that discovers the dynamic patterns of past spectrum activities to improve monitoring efficiency and reduce energy consumption within this system. In this thesis, we presented an unknown IU pattern monitoring scheme that leveraged the masses of portable mobile devices to discover the new pattern which is not included in existing incumbent users' pattern database. This scheme expanded our crowdsourcing-based existing IU pattern monitoring system at a large geographical scale and ensures our system can start to function even when no historical data is provided. It gradually created the pattern database and improved its monitoring intelligence based on the past data.

In the chapter 3, in order to prolong our system's life, we proposed a solar energy harvesting-based energy management scheme to support our spectrum monitoring system over a large

geographical area. With the LSTM-RNN network and energy management scheme that we designed, our system can accurately predict incoming solar energy and it also can work continuously during both day and night time and without running out of power and intelligently utilize the predicted solar energy. It prolongs our spectrum monitoring system's lifetime.

In the Chapter 4, we proposed an IU location privacy protection scheme under the detection of Environmental Sensing Capabilities systems. We analyzed the feasibility of preserving both static and moving IU's location by adjusting its radiation pattern and transmit power. Based on the theoretical and mathematical analysis, this thesis gives the heuristic approach and simulation results of our scheme. The simulation results show that our approach provides great effectiveness for IU's location privacy protection.

For the future work, in our crowdsourcing-based unknown IU pattern monitoring system, we only use the energy left from existing IU pattern monitoring in each T_{step} to monitor unknown IU pattern. However, since we have already known the existing pattern, the unknown pattern may be more important for us in real world (e.g., suspicious signal aware etc.). In this way, we are going to expand our system to decide which kind of spectrum to monitor at beginning of each monitoring task by calculating and determining the weight of each pattern.

For our security protection strategy, we provided the analysis for incumbent users to preserve their location privacy against ESCs. In our future work, we consider to use our protection strategy on not only incumbent users but also more general kinds of wireless nodes to protect their information security.

Chapter 6

Summary

With the widespread use of Dynamic Spectrum Access, spectrum access technology and the security of spectrum users are becoming prominent issues for exploration. In 3.5 GHz, we proposed a crowdsourcing-based unknown incumbent user's pattern monitoring scheme which enable our system to start to function even when no historical data is provided. We also proposed a LSTM-RNN to accurately predict incoming solar energy and our solar energy management schemes can guarantee the system's functionality no matter whether there is any harvestable solar power or not. We also designed novel schemes to preserve both static and moving IU's location information by adjusting IU's radiation pattern and transmit power. We first formulate IU privacy protection problem for static IU. Due to the intractable nature of this problem, in this thesis, we propose a heuristic approach based on sampling. We also formulate the privacy protection problem for moving IUs, in which two cases are analyzed: (1) protect IUs moving traces; (2) protect its real-time current location information. Our analysis provides insightful advice for IU to preserve its location privacy against ESCs. Simulation results in this thesis show that our approach provides great protection for IUs location privacy.

Bibliography

[1] United states frequency allocations: The radio spectrum. https://www.ntia.doc.gov/files/ntia/publications/january_2016_spectrum_wall_chart.pdf.

[2] S Roy, K Shin, A Ashok, M McHenry, G Vigil, S Kannam, and D Aragon. Cityscape: A metro-area spectrum observatory. In *Computer Communication and Networks (ICCCN), 2017 26th International Conference on*, pages 1–9. IEEE, 2017.

[3] Spectrum Efficiency Working Group et al. Report of the spectrum efficiency working group. *Federal Communications Commission, Tech. Rep*, 2002.

[4] Qing Zhao and Brian M Sadler. Dynamic spectrum access: Signal processing, networking, and regulatory policy. *arXiv preprint cs/0609149*, 2006.

[5] Min Song, Chunsheng Xin, Yanxiao Zhao, and Xiuzhen Cheng. Dynamic spectrum access: from cognitive radio to network radio. *IEEE Wireless Communications*, 19(1), 2012.

[6] Kang G Shin, Hyoil Kim, Alexander W Min, and Ashwini Kumar. Cognitive radios for dynamic spectrum access: from concept to reality. *IEEE Wireless Communications*, 17(6), 2010.

[7] Thao T Nguyen, Anirudha Sahoo, Michael R Souryal, and Timothy A Hall. 3.5 ghz environmental sensing capability sensitivity requirements and deployment. In *Dynamic Spectrum Access Networks (DySPAN), 2017 IEEE International Symposium on*, pages

1–10. IEEE, 2017.

[8] Yanzhi Dou, He Li, Kexiong Zeng, Jinshan Liu, Yaling Yang, Bo Gao, and Kui Ren. Preserving incumbent users' privacy in server-driven dynamic spectrum access systems. In *2016 IEEE 36th International Conference on Distributed Computing Systems (ICDCS)*, pages 729–730. IEEE, 2016.

[9] Saman T Zargar, Martin BH Weiss, Carlos E Caicedo, and James BD Joshi. Security in dynamic spectrum access systems: A survey. 2009.

[10] Rishbiya Abdul Gafoor, Riya Kuriakose, M Sibila, CK Lakshmi, S Reshmi, and Ashok S Kumar. A survey on traditional and advanced spectrum sensing techniques in cognitive radio networks. In *2018 International Conference on Control, Power, Communication and Computing Technologies (ICCPCCT)*, pages 65–72. IEEE, 2018.

[11] Deyu Zhang, Zhigang Chen, Ju Ren, Ning Zhang, Mohamad Khattar Awad, Haibo Zhou, and Xuemin Sherman Shen. Energy-harvesting-aided spectrum sensing and data transmission in heterogeneous cognitive radio sensor network. *IEEE Transactions on Vehicular Technology*, 66(1):831–843, 2017.

[12] Behnam Bahrak, Sudeep Bhattarai, Abid Ullah, Jung-Min Park, Jeffery Reed, and David Gurney. Protecting the primary users' operational privacy in spectrum sharing. In *Dynamic Spectrum Access Networks (DYSPAN), 2014 IEEE International Symposium on*, pages 236–247. IEEE, 2014.

[13] Long Zhang, Chenliaohui Fang, Yi Li, Haojin Zhu, and Mianxiong Dong. Optimal strategies for defending location inference attack in database-driven crns. In *Communications (ICC), 2015 IEEE International Conference on*, pages 7640–7645. IEEE, 2015.

[14] Yanzhi Dou, He Li, Kexiong Curtis Zeng, Jinshan Liu, Yaling Yang, Bo Gao, and Kui Ren. Preserving incumbent users privacy in exclusion-zone-based spectrum access systems. In *Distributed Computing Systems (ICDCS), 2017 IEEE 37th International*

Conference on, pages 2486–2493. IEEE, 2017.

[15] He Li, Yanzhi Dou, Chang Lu, Doug Zabransky, Yaling Yang, and Jung-Min Jerry Park. Preserving the incumbent users location privacy in the 3.5 ghz band. In *2018 IEEE International Symposium on Dynamic Spectrum Access Networks (DySPAN)*, pages 1–10. IEEE, 2018.

[16] Pradeep Reddy Vaka, Sudeep Bhattarai, and Jung-Min Park. Location privacy of non-stationary incumbent systems in spectrum sharing. In *Global Communications Conference (GLOBECOM), 2016 IEEE*, pages 1–6. IEEE, 2016.

[17] Sudeep Bhattarai, Jung-Min Jerry Park, Bo Gao, Kaigui Bian, and William Lehr. An overview of dynamic spectrum sharing: Ongoing initiatives, challenges, and a roadmap for future research. *IEEE Transactions on Cognitive Communications and Networking*, 2(2):110–128, 2016.

[18] Yanzhi Dou, Kexiong Zeng, He Li, Yaling Yang, Bo Gao, Kui Ren, and Shaoqian Li. $\hat{p}\{2\}$-sas: Privacy-preserving centralized dynamic spectrum access system. *IEEE Journal on Selected Areas in Communications*, 35(1):173–187, 2017.

[19] Lixin Shi, Paramvir Bahl, and Dina Katabi. Beyond sensing: Multi-ghz realtime spectrum analytics. In *NSDI*, pages 159–172, 2015.

[20] Ana Nika, Zhijing Li, Yanzi Zhu, Yibo Zhu, Ben Y Zhao, Xia Zhou, and Haitao Zheng. Empirical validation of commodity spectrum monitoring. In *Proceedings of the 14th ACM Conference on Embedded Network Sensor Systems CD-ROM*, pages 96–108. ACM, 2016.

[21] Jeff Howe. *Crowdsourcing: How the power of the crowd is driving the future of business.* Random House, 2008.

[22] Thomas D LaToza and Andre van der Hoek. Crowdsourcing in software engineering: Models, motivations, and challenges. *IEEE software*, 33(1):74–80, 2016.

[23] Ana Nika, Zengbin Zhang, Xia Zhou, Ben Y Zhao, and Haitao Zheng. Towards commoditized real-time spectrum monitoring. In *Proceedings of the 1st ACM workshop on Hot topics in wireless*, pages 25–30. ACM, 2014.

[24] Damian Pfammatter, Domenico Giustiniano, and Vincent Lenders. A software-defined sensor architecture for large-scale wideband spectrum monitoring. In *Proceedings of the 14th International Conference on Information Processing in Sensor Networks*, pages 71–82. ACM, 2015.

[25] Mariya Zhivkova Zheleva, Ranveer Chandra, Aakanksha Chowdhery, Paul Garnett, Anoop Gupta, Ashish Kapoor, and Matt Valerio. Enabling a nationwide radio frequency inventory using the spectrum observatory. *IEEE Transactions on Mobile Computing*, 17(2):362–375, 2018.

[26] Miguel López Benítez. *Spectrum usage models for the analysis, design and simulation of cognitive radio networks*. Universitat Politècnica de Catalunya, 2011.

[27] Leydy Johana Hernández Viveros, Danilo Alfonso López Sarmiento, and Nelson Enrique Vera Parra. Modeling and prediction primary nodes in wireless networks of cognitive radio using recurrent neural networks. 2018.

[28] Mariya Zheleva, Ranveer Chandra, Aakanksha Chowdhery, Ashish Kapoor, and Paul Garnett. Txminer: Identifying transmitters in real-world spectrum measurements. In *Dynamic Spectrum Access Networks (DySPAN), 2015 IEEE International Symposium on*, pages 94–105. IEEE, 2015.

[29] Miguel López-Benítez and Fernando Casadevall. Time-dimension models of spectrum usage for the analysis, design, and simulation of cognitive radio networks. *IEEE transactions on vehicular technology*, 62(5):2091–2104, 2013.

[30] Sudharsan Srinivasan, Sener Dikmese, and Markku Renfors. Spectrum sensing and spectrum utilization model for ofdm and fbmc based cognitive radios. In *Signal Pro-*

cessing Advances in Wireless Communications (SPAWC), 2012 IEEE 13th International Workshop on, pages 139–143. IEEE, 2012.

[31] Cengis Hasan and Mahesh K Marina. Channel vacancy forecasting for communication-free inter-operator spectrum sharing in small cell networks.

[32] Vamsi Krishna Tumuluru, Ping Wang, and Dusit Niyato. A neural network based spectrum prediction scheme for cognitive radio. In *Communications (ICC), 2010 IEEE International Conference on*, pages 1–5. IEEE, 2010.

[33] Jae-Chern Yoo and Tae Hee Han. Fast normalized cross-correlation. *Circuits, systems and signal processing*, 28(6):819, 2009.

[34] Hubert Schreier, Jean-José Orteu, and Michael A Sutton. *Image correlation for shape, motion and deformation measurements*. Springer US, 2009.

[35] Michal Piorkowski, Natasa Sarafijanovic-Djukic, and Matthias Grossglauser. CRAWDAD dataset epfl/mobility (v. 2009-02-24). Downloaded from https://crawdad.org/epfl/mobility/20090224/cab, February 2009. traceset: cab.

[36] Daniel T Wagner, Andrew Rice, and Alastair R Beresford. Device analyzer: Understanding smartphone usage. In *International Conference on Mobile and Ubiquitous Systems: Computing, Networking, and Services*, pages 195–208. Springer, 2013.

[37] Aman Kansal, Jason Hsu, Sadaf Zahedi, and Mani B Srivastava. Power management in energy harvesting sensor networks. *ACM Transactions on Embedded Computing Systems (TECS)*, 6(4):32, 2007.

[38] Aman Kansal and Mani B Srivastava. An environmental energy harvesting framework for sensor networks. In *Proceedings of the 2003 international symposium on Low power electronics and design*, pages 481–486. ACM, 2003.

[39] Sujesha Sudevalayam and Purushottam Kulkarni. Energy harvesting sensor nodes: Survey and implications. *IEEE Communications Surveys & Tutorials*, 13(3):443–461, 2011.

[40] James M Lucas and Michael S Saccucci. Exponentially weighted moving average control schemes: properties and enhancements. *Technometrics*, 32(1):1–12, 1990.

[41] Dong Kun Noh and Kyungtae Kang. Balanced energy allocation scheme for a solar-powered sensor system and its effects on network-wide performance. *Journal of Computer and System Sciences*, 77(5):917–932, 2011.

[42] Joaquin Recas Piorno, Carlo Bergonzini, David Atienza, and Tajana Simunic Rosing. Prediction and management in energy harvested wireless sensor nodes. In *Wireless Communication, Vehicular Technology, Information Theory and Aerospace & Electronic Systems Technology, 2009. Wireless VITAE 2009. 1st International Conference on*, pages 6–10. IEEE, 2009.

[43] André Gensler, Janosch Henze, Bernhard Sick, and Nils Raabe. Deep learning for solar power forecastingan approach using autoencoder and lstm neural networks. In *2016 IEEE international conference on systems, man, and cybernetics (SMC)*, pages 002858–002865. IEEE, 2016.

[44] R Martin, Ricardo Aler, José María Valls, and Inés María Galván. Machine learning techniques for daily solar energy prediction and interpolation using numerical weather models. *Concurrency and Computation: Practice and Experience*, 28(4):1261–1274, 2016.

[45] Ahmad Alzahrani, Pourya Shamsi, Cihan Dagli, and Mehdi Ferdowsi. Solar irradiance forecasting using deep neural networks. *Procedia computer science*, 114:304–313, 2017.

[46] Haşim Sak, Andrew Senior, and Françoise Beaufays. Long short-term memory recurrent neural network architectures for large scale acoustic modeling. In *Fifteenth annual conference of the international speech communication association*, 2014.

[47] Yangqing Jia, Evan Shelhamer, Jeff Donahue, Sergey Karayev, Jonathan Long, Ross Girshick, Sergio Guadarrama, and Trevor Darrell. Caffe: Convolutional architecture for

fast feature embedding. In *Proceedings of the 22nd ACM international conference on Multimedia*, pages 675–678. ACM, 2014.

[48] Diederik P Kingma and Jimmy Ba. Adam: A method for stochastic optimization. *arXiv preprint arXiv:1412.6980*, 2014.

[49] Howard J Diamond, Thomas R Karl, Michael A Palecki, C Bruce Baker, Jesse E Bell, Ronald D Leeper, David R Easterling, Jay H Lawrimore, Tilden P Meyers, Michael R Helfert, et al. Us climate reference network after one decade of operations: Status and assessment. *Bulletin of the American Meteorological Society*, 94(4):485–498, 2013.

[50] Jesse E Bell, Michael A Palecki, C Bruce Baker, William G Collins, Jay H Lawrimore, Ronald D Leeper, Mark E Hall, John Kochendorfer, Tilden P Meyers, Tim Wilson, et al. Us climate reference network soil moisture and temperature observations. *Journal of Hydrometeorology*, 14(3):977–988, 2013.

[51] Strahinja Janković and Lazar Saranovac. Improving energy usage in energy harvesting wireless sensor nodes using weather forecast. In *Telecommunication Forum (TELFOR), 2017 25th*, pages 1–4. IEEE, 2017.

[52] S Joshi, KBS Manosha, M Jokinen, T Hänninen, Pekka Pirinen, H Posti, and M Latva-aho. Esc sensor nodes placement and location from moving incumbent protection in cbrs. In *Proceedings of WInnComm 2016*, 2016.

[53] Federal Communications Commission et al. Wireless telecommunications bureau and office of engineering and technology establish procedure for registering environmental sensing capability sensors. *FCC Public Notice*, 2018.

[54] Han Xiao, Hao Zhang, Zengfeng Wang, and T Aaron Gulliver. An rssi based dv-hop algorithm for wireless sensor networks. In *Communications, Computers and Signal Processing (PACRIM), 2017 IEEE Pacific Rim Conference on*, pages 1–6. IEEE, 2017.

[55] Jiang Xiao, Zimu Zhou, Youwen Yi, and Lionel M Ni. A survey on wireless indoor

localization from the device perspective. *ACM Computing Surveys (CSUR)*, 49(2):25, 2016.

[56] Ting Wang and Yaling Yang. Analysis on perfect location spoofing attacks using beamforming. In *INFOCOM, 2013 Proceedings IEEE*, pages 2778–2786. IEEE, 2013.

[57] Roberto Vescovo. Pattern synthesis with null constraints for circular arrays of equally spaced isotropic elements. *IEE Proceedings-Microwaves, Antennas and Propagation*, 143(2):103–106, 1996.